
# REMOTE CONTROLLED DRUG RELEASE IN DRUG-ELUTING STENTS

**Noor Al-Nasser (201271063)**

2012/2013

University of Strathclyde, Department of Biomedical Engineering

This thesis is submitted in partial fulfilment of the requirements for the degree of Masters of Science in the Biomedical Engineering Unit

**Declaration of Authenticity and Author's Rights**

‘This thesis is the result of the author’s original research. It has been composed by the author and has not been previously submitted for examination which has led to the award of a degree.’



Signed: Date:

**Acknowledgements**

بـ سم الله الـ رحمن الـ رحـ يم

I would like to personally thank the Department of Biomedical Engineering, University of Strathclyde, to all the staff and students of class 2012-2013. It has been a thoroughly enjoyable year that I will always remember, and I wish everyone the very best.

For this thesis, I thank Dr. Wei Yao for his creativeness and visionary, and for allowing me to partake in a thought provoking project, and for the support throughout the summer. And to Dr. Christopher McCormick, who was there in my times of need.

This project would not have been possible without the help from the Photophysics department. I personally thank Dr. Yu Chen for the knowledge and expertise you provided me, and to PhD student Peng Gu, whom I pestered on many occasions, I thank you for your support within the laboratory and I wish you all the best in your studies and future.

I wholeheartedly thank all my family and friends for their patience, love and support throughout the entire year.

God bless.

**Abstract**

Coronary artery disease is one of the most predominant types of heart diseases present in the 21st century, attributing to a staggering 7.2 million deaths annually across the globe [1]. After implantation of currently the most successful coronary intervention, drug-eluting stents are placed within obstructive arteries to restore blood flow to the heart and reverse life-threatening consequences. However, it is still plagued by the resurrection of artery occlusion, resulted by stent-induced restenosis.

This battling and persistent problem is of complex aetiology, even with the incorporation of anti-proliferative drugs. One of the key flaws resulting in the restenosis is denying the arterial wall time to heal after implantation due to the sequential drug release. Introducing a novel smart drug delivery system onto stents can enable the release of drug locally in a controlled manner by means of an external ultrasonic stimulus. This ultrasonic-triggered drug release can be tailored to the needs of individuals and controlled within the hands of the cardiologist, to maximise drug efficacy and patient outcome.

**Table of Contents**

**List of Abbreviations**

| | |
|---|---|
| ACE | angiotensin-converting enzyme |
| AuNP | gold nanoparticles |
| BMS | bare metal stent |
| CABG | coronary artery bypasses graft |
| CAD | coronary artery disease |
| CCB | calcium channel blockers |
| Co-Cr | cobalt chromium |
| CVD | cardiovascular disease |
| DES | drug-eluting stent |
| DS | dextran sulphate |
| EES | everolimus-eluting stent |
| EGFR | epidermal growth factor receptor |
| EPD | electrophoretic deposition |
| ISR | in-stent restenosis |
| LbL | layer-by-layer |
| LST | late stent thrombosis |
| MRI | magnetic resonance imaging |
| OSIRIS | oral sirolimus to inhibit recurrent in-stent restenosis |
| PAA | polyacrylic acid |
| PAH | poly(allylamine hydrochloride) |
| PCI | percutaneous coronary intervention |

| | |
|---|---|
| PDA | poly(diallyldimethylammonium chloride) |
| PE | polyelectrolyte |
| PEI | polyethylenimine |
| PES | paclitaxel-eluting stent |
| PLA | polylactic acid |
| PSS | poly(styrene sulfonate) |
| rpm | rotations per minute |
| SEM | scanning electron microscope |
| SES | sirolimus-eluting stent |
| SMC | smooth muscle cell |
| SPR | surface plasmon resonance |
| WHO | world health organisation |
| ZES | zotarolimus-eluting stent |

**List of Figures**

**List of Tables**

# 1 Introduction

In accordance to some of the major global health organisations, including the World Health Organisation (WHO), American Heart Association and European Public Health Alliance, the primary leading cause of disability and mortality in both the developed and developing world is caused by cardiovascular diseases (CVDs). An estimated 17.3 million deaths were attributed to CVDs in 2008, representing almost a third of all global deaths [1]. These include those directly affecting the cardiovascular system, including; primarily cardiac diseases, vascular diseases of the brain and kidneys, and peripheral arterial diseases. Statistical evidence shows an overwhelming rise in cases, with a predicted mortality rate of 23.3 million by 2030 [1]. This global scale problem places demands for newer, more effective and more advancing cardiovascular devices to compete with these accelerating rates.

One of the most common types of CVD is coronary artery disease (CAD). The result of stenosis in the coronary artery is due to accumulative atherosclerotic plaque obstructing the blood flow supply of heart, depriving oxygen and nutrients to the cardiac muscle. The placement of drug-eluting stents (DESs) in diseased coronary arteries aims to resolve the consequences caused by stenosis. The slow and continuous release of drug from the polymer-coated stent begins almost instantly after implantation, for a period of up to 90 days. This anti-proliferative drug, such as paclitaxal or siroliumus, prevents the neointimal growth caused by smooth muscle cell (SMC) proliferation effectively. Restenosis is reduced compared to other minimally invasive techniques. However, the inhibiting drug also deprives the growth of new endothelial layers, an impediment to the healing of the arterial wall. This prevention increases the risk of in-stent restenosis (ISR).

In a different field of therapeutics, the use of nanotechnology for drug delivery has become a promising tool for the future; a sophisticated method which can be modified to suit the needs of the individual. Advanced drug delivery systems have seen the use of drug encapsulation, which uses the concept of micropackaging small drug molecules within macroscale biocompatible shells, which are then injected into the circulatory system. The drug release from inside these shells can be controlled

either by an internal or external stimulus. Externally, the source can be by laser irradiation, ultrasound or a magnetic field. Once these circulating drug-encapsulated shells reach the location of injury, intense energy is directly aimed on site to rupture the shell to release the drug locally, giving optimal results (Antipina and Sukhorukov, 2011). Its varying applications have been given a great deal of research over the past decade, with its application intended for cancer therapy to optimise treatment of tumour ablation, and in other techniques for organ specific gene and drug delivery.

## 1.1 Thesis Objectives

The objective of this project is to introduce a new innovative concept; to combine both these therapeutic systems together. Supported by the literature review, the idea is to incorporate an advanced drug delivery system of encapsulated drugs onto DES, which is later subjected to an external ultrasonic stimulus for drug release. The proposed delivery vehicle is polyelectrolyte (PE) microcapsules, a useful technique for encapsulating water-soluble drugs, which will be investigated in the methods.

Success of this will permit drug release from the stent in a controlled manner within a particular time frame and impede disadvantages previously conceived by DESs. Drug release inhibition in the early days of implantation will allow the formation of a new endothelial layer to form over the stent, healing the arterial wall and secure the stent in place before triggering the drug release to inhibit the SMC proliferation. Such a feature will give the interventional cardiologist more control of the medical implant.

The results and discussion of the experimental procedure will interpret the findings and digress into the challenges faced and possible alternative solutions. Following this, suggestions will be made in terms of future work. To conclude, it is hoped that this concept can justify its potential and potent need in clinical practice and can be taken forward in future.

# 2 Literature Review

## 2.1 Introduction

The field of biomedical engineering is further pushing the boundaries to design the next generation of medical systems and treatments, advancing the quality of life for patients. For this, the understanding of the disease aetiology and fundamental components of the assisting medical device must be appreciated. This section will focus on CAD and their clinical therapeutic options, the limitations faced, and introduce a novel drug delivery system currently gaining interest as a new therapeutic technique.

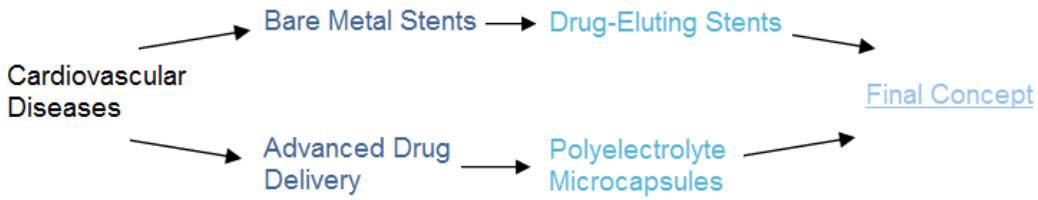


**Figure 2.1:** Schematic flow-diagram overview of the literature review.

## 2.2 Coronary Artery Diseases

The coronary circulation is a system of blood vessels responsible for supplying oxygen-rich blood to the myocardium (cardiac muscle). As the left and right coronary arteries branch out from the ascending aorta and run across the surface of the heart, these epicardial coronary arteries under normal physiological conditions have an auto-regulative mechanism. This maintains suitable blood flow levels relative to the requirements of the cardiac muscle, whether in a rested state or under physical stress. The walls of healthy epicardial coronary artery consist of three layers; the tunica intima, tunica media and tunica externa.

CAD is a chronic process contributing to 41% of all CVD cases [1]. Comparatively narrower than other arteries, the coronary arteries are susceptible to atherosclerosis; where atherosclerotic deposits accumulate to form calcified plaques. This degenerative disease first begins with the development of fatty streaks comprised of atherogenic lipoproteins and macrophage foam cells, which form between the endothelium and internal lamina. Over a prolonged time (up to years), an intermediate lesion of SMCs and connective tissue matrix then layers over the fatty streaks, forming a fibrous cap. This now poses high risks to the individual, predominantly at the edges of the fibrous cap since plaques can lose stability and ruptures. Should the plaque rupture, the underlying thrombogenic core is exposed to the circulating blood, resulting in the accumulation and aggregation of platelets and other blood components and imminently cause total occlusion of the artery. This causes one of the most serious consequences, as it can initiate a cardiac arrest which may result in death.

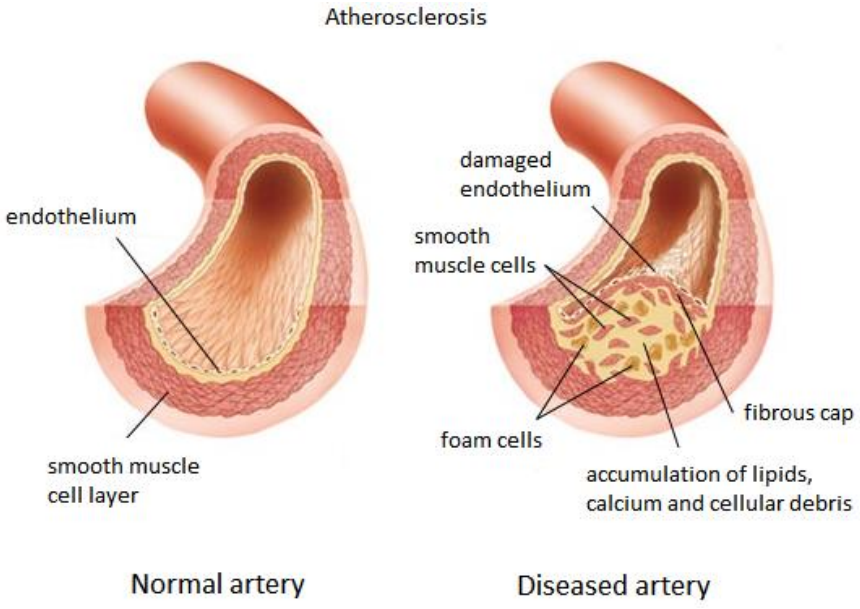


**Figure 2.2: Comparison between a healthy and diseased artery;**
*Left*: The inner intima layer surrounds the lumen of the blood vessel; the media is the thickest containing layers of SMC and elastic fibres and the externa is composed of mainly elastic and collagen fibres.
*Right*: Atherosclerosis occurs when the intima becomes damaged, initiating a cascade of events, resulting in an atherosclerotic plaque. Reduced luminal area restricts blood flow [2].

The treatments used for CAD is dependent on the symptoms and the severity of the condition. Associated risk factors include obesity and lack of exercise, tobacco use, hypertension and hyperlipidaemia. Therefore, it is strongly advised that once diagnosed with CAD, or any other heart disease, committed lifestyle changes should be made by addressing these risk factors. However, these changes alone may not be sufficient.

### *2.2.1 Medical treatments*

Pharmaceutical medicines can be prescribed when atherosclerosis is identified at an early stage to prevent further complications and ease the symptoms. Cholesterol-lowering statin drugs decreases the amount of low-density lipoprotein circulating in the blood- the primary material that deposits in the coronary artery; whereas angiotensin-converting enzyme (ACE) inhibitors (which decreases blood pressure) and beta-blockers (slows heart rate and decrease blood pressure / oxygen use) prevent and reduce the risk of future heart attacks [3].

Furthermore, nitrates dilate the arteries for increased blood flow, calcium channel blockers (CCB) relax the surrounding cardiac muscles of the coronary artery, as well as a daily dose of aspirin to reduces the tendency of blood clots, may be alternatively recommended. If these drugs used alone or in combination become ineffective, then more aggressive forms of treatments is needed.

### *2.2.2 Surgical interventions*

When several diseased coronary arteries become unresponsive to any treatment, or if the patient is at high risk of lesions or multiple vessel disease, coronary artery bypass graft (CABG) surgery is implemented. This type of arterial revascularisation is to re-establish the coronary blood flow to the myocardium by creating a graft that bypass the blocked artery using a vessel taken elsewhere from the patient's body, thus creating a new passage of blood flow. The conduits used for bypass are the internal thoracic artery, the radial artery (forehand), and the saphenous vein (leg). First introduced successfully in 1960 by surgeon Robert H. Goetz and his team (Lubell,

2002), the procedure rapidly became the standard of care for symptomatic patients with CAD. With emerging advances in coronary surgery in the later years, it had reduced the rate of morbidity, mortality and graft occlusion. However, the advent of new minimally-invasive and non-surgical techniques, such as angioplasty and coronary-stent implantation, has seen it competing and overtaking CABG surgery.

## 2.3 Bare Metal Stents

Percutaneous coronary intervention (PCI), or balloon angioplasty, has rapidly become an appealing alternative to the more invasive surgical techniques. 88,700 procedures were performed in 2011 in the UK alone [4], compared to 28,000 for CABGs [5]. Prior to the procedure, a coronary angiogram is performed to investigate sites of any narrowing or blockages, and if determined, an intervention will follow. PCI involves the insertion of a thin flexible catheter through a small incision in the femoral or radial artery. A balloon, attached to the end of the catheter, is guided towards the obstructed coronary artery. On site, the balloon is inflated, compressing the atherosclerotic plaque up against the arterial wall. The balloon catheter is removed from the body; leaving behind an expanded lumen diameter and restored blood flow. Revascularisation using this procedure has been successful since its introduction; however, it later became evident that the technique was limited by two factors. First, elastic recoil of the vessel attributed to a significant loss of luminal area after balloon angioplasty, increasing the risk of arterial blockage within a very short period of time. The second limitation is the remodelling process of the artery which came in the later weeks and months following the procedure, resulting in a luminal area loss of greater than 50% due to the return of stenosis (restenosis) (Haude *et al.,* 1993).

At present, almost 92% of all PCI procedures are now assisted by stents to overcome the limiting factors conceived by PCI alone [4]. Bare metal stents (BMS) are small, tubular, wire-meshed devices designed to have the mechanical strength to act as a scaffold to the artery. Similar to the procedure for PCI, the BMS is mounted onto the balloon catheter in a crimped form, to allow easier delivery. When the balloon is inflated on site, the metal stent is expanded, providing permanent support and

prevent immediate elastic recoil. This technique has now been utilised in clinical practice for over 20 years for obstructive coronary arteries (Martin and Boyle, 2011). However, albeit improving patient outcomes in terms of chest pain and quality of life, this technique is still plagued with restenosis, but in this case, ISR; the re-narrowing of the artery after stent implantation.

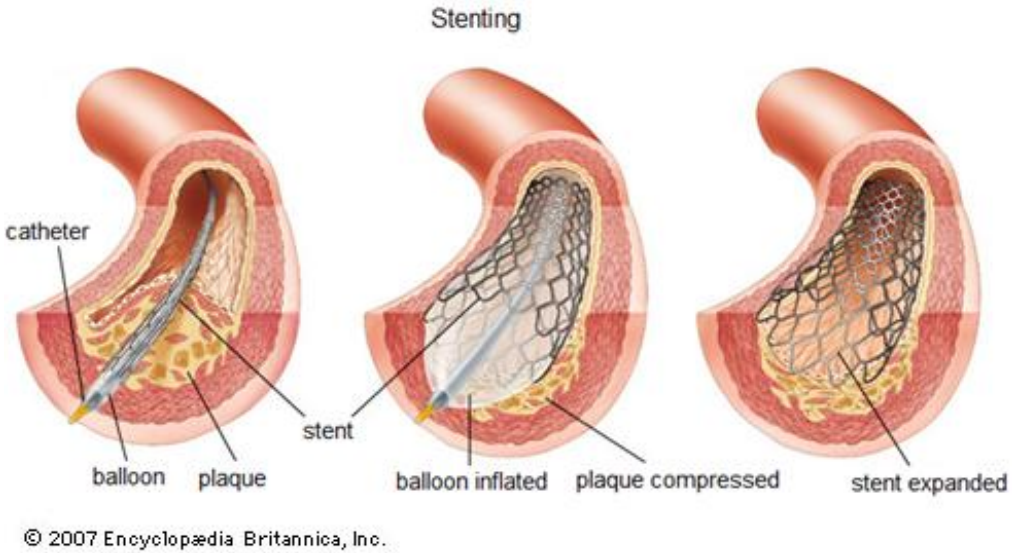


**Figure 2.3: Stent procedure within the diseased coronary artery;**
*Left:* Balloon catheter with stent guided to the atherosclerotic site within the artery.
*Middle:* Balloon is inflated causing expansion of stent and compression of plaque.
*Right:* Balloon catheter is removed, leaving the stent in place for mechanical support. Blood flow is restored [6].

### *2.3.1 Stent design*

One of key element in optimising the application of coronary stents is the selection of a biologically inert material. The material determines the most essential aspects of the stent's performance, including the mechanical, surface, and corrosion properties. Good mechanical properties are based on the material's elastic modulus, the tensile strength and elongation, whereas the surface properties can possess electrical charge and different textures. Corrosion is associated with the deterioration of the material within the biological environment, and leeching of metal ions can deem toxic to the surrounding tissue (Lévesque *et al.*, 2004).

Commonly used 316L stainless steel provides good mechanical properties of strength and flexibility, and is corrosion resistant. However, the iron components cause artefacts during magnetic resonance imaging (MRI), and deliverability is challenging due to the poor visibility. Nickel components too can cause issues by triggering allergic reactions which may accelerate restenosis. Cobalt chromium (Co-Cr) alloy is also used as a stent material, which is radiopaque and MRI-compatible. With high radial strength, struts are made thinner than stainless steel stents, without compromising vascular support. Other lesser used materials include nitinol shape-memory alloy, magnesium alloy and platinum, but these usually require thicker struts due to their poorer radial strength.

Alongside the mechanical properties contributing to the strength, the design of the stent is also critical, as it needs to obtain sufficient radial strength to hold the vessel open. Over the years, the design has gone through several different designs to reach an optimal balance of mechanical strength and flexibility. Flexibility, another key aspect of the design, allows the stent to be delivered percutaneously within the vasculature of small vessels, which can be of intricate geometry. This is also determined by the strut thickness; thicker struts provide more support, whereas thinner struts increases flexibility and deliverability of the stent, and contribute to less damage to the arterial wall. Stents are either laser-cut from a slotted tube or welded together using repeated units of sinusoidal-formed wires. While both have high radial strength, the latter maximises flexibility.

### *2.3.2 In-stent restenosis*

The complexity of ISR that follow stent implantation is implicated by an iatrogenic aetiology, which can be as high as 48% of the BMS population (Mohan and Dhall, 2010). This restenosis of the treated artery is burdened with molecular, physiological and biochemical reactions, and is defined as a stenotic diameter of 50% or greater of the initial stented vessel (Martin and Boyle, 2011). In some cases, BMSs in the coronary artery triggers a cascade of highly interrelated pathways which result in neointimal hyperplasia, leading to the re-narrowing of the artery lumen. This is more frequently observed in patients with other underlying diseases such as diabetes, or

those presenting particular lesion characteristics or complex lesion geometries, and this limits the treatment efficacy of stents.

Several key pathways contribute to the development of the neointimal layer. Once the stent is deployed in the artery, a lesion is formed in the endothelium which results in thrombus formation and the adhesion and aggregation of activated platelets (Kamath *et al.*, 2006). These inflammatory responses now cause vascular SMC proliferation and migration from the media to the intima of the artery. Combined with an altered matrix metabolism of the extracellular matrix (Farb *et al.*, 2001), this contributes to the remodelled and narrowed artery wall. The vascular injury following stenting resembles the events in general wound healing; formation of scar-like tissue. The compromised pathophysiology of the artery now makes the biological environments for any subsequent interventional procedure very challenging (Kamath *et al.*, 2006).

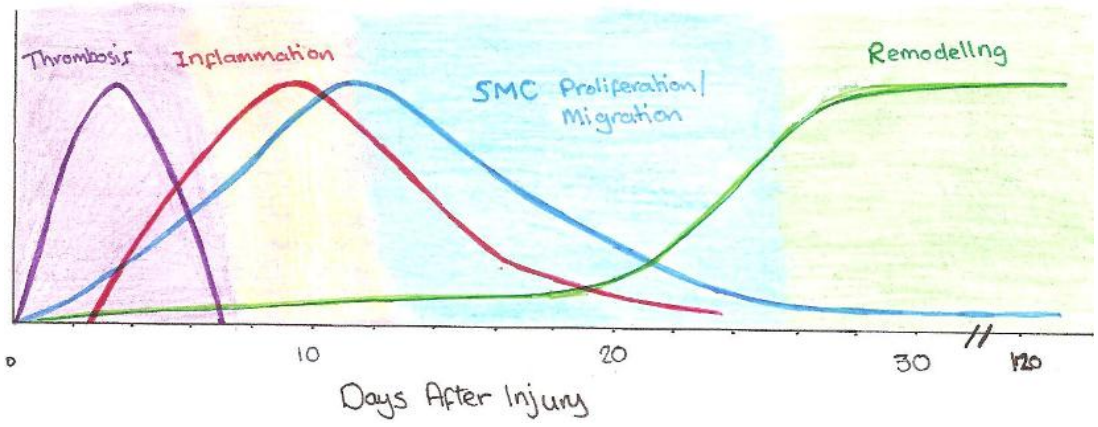


**Figure 2.4: Schematics representing the cascade events of ISR after stent-induced arterial injury;** Platelet adhesion and aggregation/thrombus formation (purple); inflammatory responses initiating leukocyte recruitment (monocytes, macrophages) (red); SMC proliferation and migration (blue); remodelling of the ECM due to matrix deposition and healing process (green). Adapted from Kamath *et al.*, (2006).

A variety of oral systemic therapeutics have been identified in preventing ISR, including; ACE inhibitors, statins, CCBs, vitamins and anti-proliferative drugs. Anti-platelet and anticoagulant drugs have been used, targeting the platelets and thrombi which initiate the cascade of events of neointimal proliferation (Schömig *et al.*, 2005). Albeit the initial improved outcomes, their use does not reduce the rate of neointimal hyperplasia and restenosis, which is also replicated in some of the above-mentioned therapeutics, whereas ACE inhibitors and vitamins have led to conflicted reports (Schömig *et al.*, 2005). To date, the most successful drugs are aspirin and heparin, which exhibit anti-platelet and anti-thrombotic characteristics respectively.

Ultimately, these systemic treatment approaches have shown limited efficacy in reducing ISR, primarily due to the lack of site-specific targeting of right mechanism with the most effective drug during the right time. In regards to this, sirolimus was used in a randomised OSIRIS (oral sirolimus to inhibit recurrent ISR) study, by using a double-blinded and placebo-controlled trial. The anti-inflammatory and anti-proliferative drug yielded positive results and effectively reduced ISR with short term-treatment (Schömig *et al.*, 2005).

Furthermore, the OSIRIS trial also indicated the positive outcomes when administrating a sufficient drug dose prior to stent implantation. Patients who received a high dose of sirolimus prior to stenting had improved outcomes, in terms of angiographic and clinical restenosis (Schömig *et al.*, 2005). This suggests that sirolimus may be effective during the early days of implantation since it targets the critical events that contribute to neointimal formation.

## 2.4 Drug-Eluting Stents

To tackle the battling issue of ISR, the past decade has seen the introduction of DESs, receiving CE and FDA approval in 2002 and 2003 respectively (Martin and Boyle, 2011). Previously dominated by BMS, DESs have revolutionised the field of interventional cardiology, becoming the newest treatment modality available to the cardiologist. DESs is supported by a powerful demonstration of clinical success; treating more complex lesions that would otherwise require invasive surgical CABG, as well as reducing the need for repeated revascularisation due to improved patient care (Kamath *et al.,* 2006; Chitkara and Gershlick, 2010). Simply put, the new additional aspects applied to a standard BMS frame are the active drug formulation and a polymer carrier, to achieve a final therapeutic outcome of an implant-based local drug delivery system (Kamath e*t al.,* 2006).

Any mechanical injury sustained during the stent implantation triggers the healing response of the vessel, resulting in neointimal growth. To date, only a handful of anti-restenotic drugs have shown clinical effectiveness under evaluation, which disrupt the key cellular and molecular processes involved with the proliferative effects of ISR. This has led to the evolution of first-generation DESs; Cypher sirolimus-eluting stent (SES) and Taxus paclitaxel-eluting stent (PES), both utilising a 316L stainless steel stent. The drug mechanism of SES is designed to release approximately 80% of the drug within the first 30 days of implantation (Martin and Boyle, 2011). For PES, however, there is a short burst of release within the first 48 hours, followed by low-level release over the following 10 days (Martin and Boyle, 2011).

The introduction of Co-Cr stents led to the development of two second-generation DESs using more effective drugs. Endeavor zotarolimus-eluting stent (ZES) releases approximately 95% of the total dose of zotarolimus within the first 15 days of stent placement (Martin and Boyle, 2011). The second is Xience-V everolimus-eluting stent (EES), where the release profile of everolimus replicates SES.

Since obtaining CE and FDA status, both first and second generation DESs have been evaluated in many clinical studies to assess their safety and efficacy when deployed in a number of patient and lesion sub-groups. Furthermore, NICE have implemented guidelines on their use in clinical practice, stating that DESs should only be implemented as a possible treatment to those presenting an affected coronary artery of less than 3mm in diameter, or the affected section is no longer than 15mm, combined with the additional cost over BMSs of less than £300 [2].

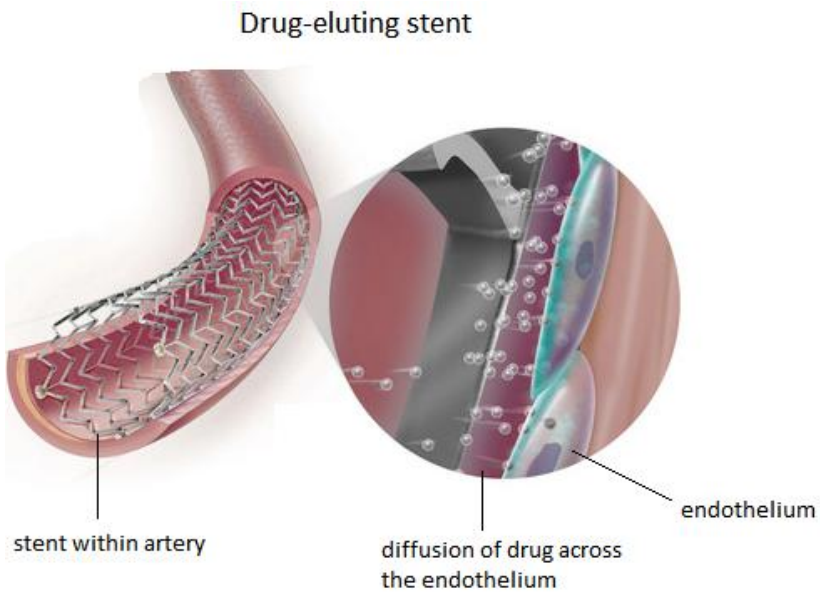


**Figure 2.5: Drug release from a drug-eluting stent;** Diffusion of drug molecules from the DES across the arterial wall, ensuring maximum delivery of therapeutic directly to target site [7].

### *2.4.1 Drug release mechanisms*

The controlled release mechanisms of the anti-restenotic drug in DESs are by means of chemical or physical mechanisms. Physical mechanisms have the advantage of designing the delivery system to control the drug release kinetics. This can be done by altering specific parameters, including the type of polymer, the thickness of the coating, and the dimension of the exposed surface area. Chemical mechanisms have

disadvantages due to the contamination of new chemical entities during chemical modification of the drug (Acharya and Park 2006).

| Mechanism of controlled drug release | Properties of mechanism |
|---|---|
| **Diffusion** | Drug molecules are released by diffusion through the polymer layer either via a reservoir or matrix system |
| **Dissolution or degradation** | Drug release based on dissolution or degradation of the polymer matrix, controlling the drug release |
| **Ion exchange** | Used for ionised drugs which bind to matrix through electrostatic interactions |
| **Osmosis** | Increase of osmotic pressure inside the device causes drug release |
| **Prodrug (chemical)** | Chemical or enzymatic degradation break the covalent bonds that connect drug molecules to delivery vehicle |

**Table 2.1:** Properties of the drug release mechanisms in current DESs.(Adapted from Acharya and Park (2006).

In the SES, ZES and EES, the release of their corresponding drug exhibit potent anti-proliferative and immunosuppressive effects. Inhibition of SMC proliferation is achieved by binding to cytosolic FK-binding protein 12. This prevents activating mammalian target of rapamycin, resulting in cell-cycle arrest in the G1 to S phase (preparation step for DNA replication) (Martin and Boyle, 2011). Drug release from PESs suppresses neointimal growth by binding and stabilising microtubules from their disassembly, rendering them non-functional. This results in the inhibition of the cell division in the G0-G1 and G2-M phases (Chitkara and Gershlick, 2010).

### *2.4.2 Limitations*

Although superior to the BMS, DESs still serves further limitations, with current debates over their safety of use. The drug platform is a thin biostable polymer of 5 - 10 µm surrounding the struts yielding low volume, small thickness, and high surface area drug delivery system. Cumulative drug release curves convey that the majority of the release occurs within the first 24 hours after implantation, and in some cases where the drug is attached directly onto the stent, almost a third is retained within the stent indefinitely (Serruys and Gershlick, 2005). Altering the release mechanisms can be difficult, as it is determined by physical and chemical properties of the drug-polymer. It is also suggested that the success and toxicity of stenting correlates to the significant and rapid release of the drug compounds into the adjacent vessel wall.

Aside from limitations due to the release effectiveness, the iatrogenic injury caused by BMS and DES also stimulates problems. Implantation causes the removal of the endothelial layer and damages the tunica media. This triggers the inflammatory response resulting in ISR, which continues to grow. Data suggest that if ISR occurs in BMS, this will be observed within the first 6 months after stent implantation, whereas it occurs much later in DESs. Depending on the lesion complexity, the rate of restenosis in DES can reach 10% in 2 years, with repeated intervention rate of 17.2% in 5 years. The rates are even higher if patients suffer from multiple vessel disease, and revascularisation can be 17.4% within 2 years (Teirstein 2010), with rates expected to rise over the coming years. Late stent thrombosis (LST) is another issue related to DES failure, reported in several cases, although uncommon. It is a blood clot formation, which can later result in artery occlusion. Unlike ISR, LST occurs years after implantation, predominantly if anti-platelet therapy is ceased.

As mentioned, damaged endothelium, which directly causes ISR and LST, required a new endothelial layer to form over the stent to avoid neointimal growth. Since the timeline of DESs prohibits and delays this, a smart drug delivery mechanism needs to be incorporated. This leads to the following section of advanced drug delivery systems, which are currently being investigated as a tool for hand-controlling the release of drugs as a novel treatment option.

## 2.5 Advanced Drug Delivery Systems

Moving away from DESs, it is important to investigate other drug delivery techniques, and appreciate their mechanisms. Understanding the science of drug delivery provides the development of individually tailored systems by chemical modification, and with advances in biology, physics and engineering, the latest progression is the ability to locally deliver therapeutic drugs to site-specific targets, controlled by internal and external stimuli.

Achieving this requires the knowledge of the evolving field of nano- science and technology; a field aiming to optimise medical approaches in clinical diagnostic and therapeutic practice. Nanoscience is described as the manipulation of matter at an atomic and molecular level. This is dependent on nanotechnology; its production at a nanometre scale, and the analysis and application into devices and systems (Vergaro *et al.* 2011). When this is implicated into biology and medicine, the application of nanotechnology is brought to new levels; from nanoscale surgery, tissue engineering, and molecular imaging, to targeted drug delivery (Vergaro *et al.* 2011).

A promising technique is the concept of drug encapsulation, where therapeutic substances of a nanometre scale (10 – 1000nm) are entrapped within biocompatible shells. These delivery vehicles are known as nanocarriers, and some of those discovered so far include lipid-based carriers, polymer conjugates, polymeric nanoparticles, albumin, carbon nanotubes and magnetic nanoparticles, such as iron tetroxide or gold. The therapeutic core inside the nanocarriers may be solid, liquid or gas, and usually comprises of a homogenous mix of polymer and active drug ingredient (Singh *et al.*, 2010). These drug carriers are responsive to different parameters of the surrounding media. This may include an internal stimulus such as temperature, pH and sugar concentration. They are also able to carry and release the encapsulated load in response to an external stimulus such as a magnetic field, light or ultrasound (Pavlov *et al.*, 2011). The biological aims are to minimise systemic toxicity by precise drug targeting and delivery, and improve safety and biocompatibility of medicines.

**Figure 2.6: Drug loading of various nanocarrier systems;**
*Left:* Liposome shell with hydrophilic (orange) and hydrophobic drugs (purple).
*Middle:* Hydrophobic drugs within a micelle.
*Right:* Hydrophilic drugs entrapped in nanogels.

## 2.6 Polyelectrolyte Microcapsules for Drug Delivery

A possible engineered solution of such a delivery system is the recently developed PE multilayered microcapsules. PEs are polymeric molecules of ionisable monomers with low molecular weight counter-ions that maintain electrical neutrality. When dispersed in aqueous solution, the monomers dissociate, and the polymer becomes charged. PE microcapsules are formed by deposition of alternatively charged PEs layers onto a core, preparing a stimuli-responsive drug carrier for targeted drug delivery.

Although the term microcapsule suggests a core with a solid shell structure, PE microcapsules are rather a dispersion of a solid matrix which lacks a definitive external wall phases. PEs can be coated onto dissolvable colloidal particles between 20nm to 50µm (Antipina and Sukhorukov, 2011), and the size of the entire microcapsule can reach up to 2000µm, distinguishing them from other smaller nanocarriers/nanocapsules. Aside from the therapeutic drugs encapsulated within the core, drugs can also be attached to the shell of the microcapsule or contained within the layers of the shell (Shi *et al.*, 2007). PE microcapsules have been introduced as an efficient drug delivery system for spontaneous encapsulation of low molecular weight water-soluble drugs, with their loading and subsequent release dependent on the permeability of the capsule wall (Anandhakumar *et al.*, 2011).

### *2.6.1 Layer-by-layer assembly*

PEs can undergo a self-assembly process known as layer-by-layer (LbL). This involves adsorbing alternatively charged polyanions such as poly(styrene sulfonate) (PSS), or dextran sulphate (DS), with polycations poly(allylamine hydrochloride) (PAH), or polyethylenimine (PEI). The method utilises the attractive electrostatic forces between the charged polymers and the oppositely charged surface. A thin layer coats the nanoparticles by the repetitive exposure to polycation and polyanion solutions (Vergaro *et al.*, 2011), repeating until reaching the desired multilayer thickness, forming a multilayered PE microcapsule of a typical size of 3 – 5µm (Pavlov *et al.*, 2011).

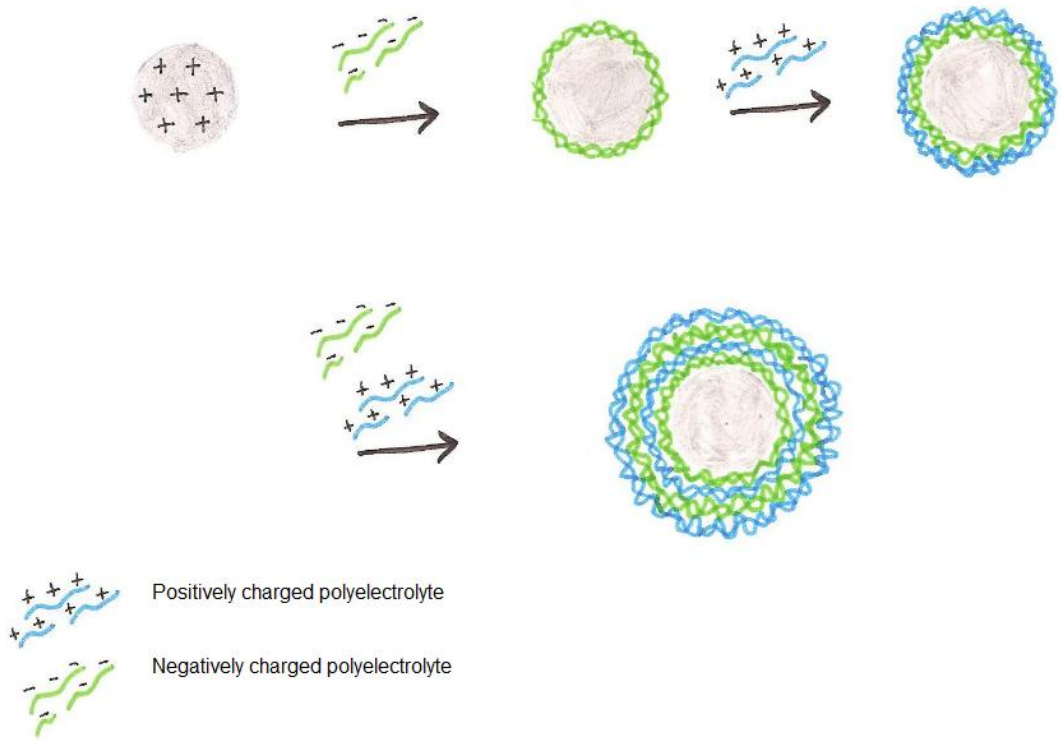


**Figure 2.7: Schematic of PE microcapsule fabrication via LbL assembly;**
Initial cationic core subjected to a negatively charged polymer, followed by a second layered coating of positively charged polymer. Multiple layers form microcapsule (not drawn to scale).

### *2.6.2 Metal nanoparticles*

Incorporating metal nanoparticles such as gold, silver, or platinum in between the soft polymeric layers of PEs adds extra functionalities to the supramolecular structures of the LbL microcapsules. Microcapsules now become more sensitive to rupturing under an external stimulus (Pavlov *et al.*, 2011); therefore, the power required can be made much lower. When microcapsules are modified with metal nanoparticles, the release of the encapsulated payload from ultrasonic triggering can be as high as 99% as reported by Skirtach *et al.*, against only 20% release from solely PE shells (Antipina and Sukhorukov, 2011). For gold nanoparticles (AuNP), there seems to be a particular interest due to its unique optical properties. The surface plasmon resonance (SPR) of a material is the collective oscillations when stimulated by incident light, and for AuNP, they contain a strong SPR signal in the visible spectrum at around 530nm (Vergaro *et al.*, 2011). Hence at this wavelength, laser irradiation cause local heating of the AuNP via conversion of photons to thermal energy, rupturing the microcapsule and releasing the encapsulated material. The SPR can be modified by altering the shape and aggregation of AuNP on the microcapsule surface, and be made reversibly permeable to infrared radiation. With this, it has been suggested that the payload can be released in portions without destroying the entire microcapsules (Vergaro *et al.*, 2011).

### *2.6.3 Ultrasound-triggered drug release*

Physical influences including magnetic field, light, and ultrasound, are widely used in clinical practice both for diagnostic and therapeutic purposes. For ultrasound, it has served therapeutically for many diseases due to its minor destructive effect, with a variety of FDA-approved ultrasonic processors and instruments available in clinics. Low frequency ultrasound of around 20 kHz is not used in medicine (except in dentistry) and combined with high power conditions, it is deemed dangerous for *in vivo* therapeutic applications due to the resulting damage to collateral tissues (Pavlov *et al.*, 2011). However, high frequencies of ~1 MHz with low power (1 - 3.5 W) is widely used in medicine for physiotherapy, treatment of diseased or injured organs, and more recently, in focused ultrasound surgery (Antipina and Sukhorukov, 2011).

In terms of drug delivery systems, an ultrasonic stimulus can be applied to stress the delivery vehicle to release the therapeutic material. This is achieved by exposing the pores of the shell, or by rupturing and breaking them down completely. Ultrasound, therefore, can be utilised as a remote controlling tool over the release of encapsulated material, which can be achieved both *in vitro* and *in vivo* (Antipina and Sukhorukov, 2011).

When subjected to ultrasound, the microcapsule wall undergoes a morphological change due to shear forces between the each fluid PE layer, due to the ultrasonic oscillations. This disruption of the microcapsule triggers the drug release. To maximise the effect, the ultrasonic wavelength of the oscillations must correlate to the microcapsule's size. Hence, the frequency dictates the energy liberated on their collapse. According to Minneart's resonance equation, when the ultrasonic frequency is 20 kHz, the wavelength in water is 7 cm and the size of the microbubble created is 150 µm. At 1 MHz, the wavelength is 1.4 mm with a microbubble size of 3 µm, much closer to the size of PE microcapsules (Pavlov *et al.,* 2011). With the introduction of a rigid material such as the AuNP, the higher amount of the embedded nanoparticles leads to a decreased Young's modulus and microcapsule shell elasticity (Antipina and Sukhorukov, 2011). This can influence the fracture rate under ultrasonic triggering, making them more vulnerable to ultrasound. In general, the goal of drug delivery and targeting is to improve efficacy of the drug action in the region of the disease whilst reducing side effects such as toxicity within healthy tissue.

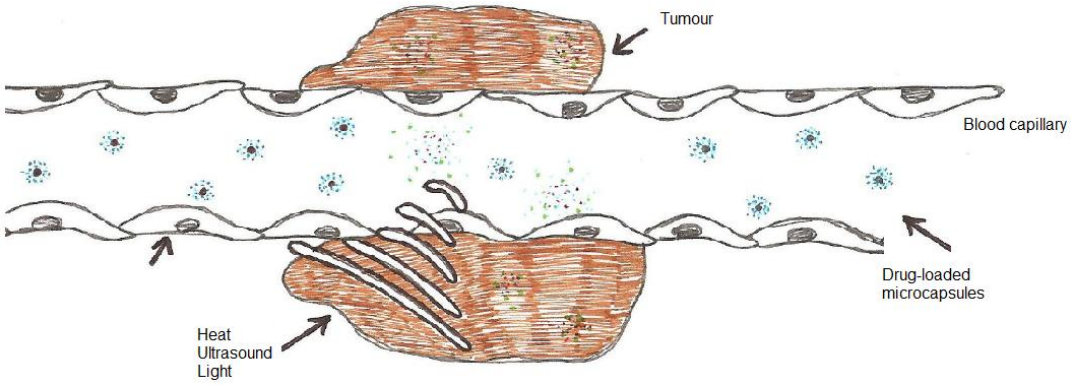


**Figure 2.8: Tumour targeting of drug-loaded PE microcapsules;** Triggered drug release from heat, light or ultrasound. Released drug molecules enter into the tumour.

## 2.7 Remote controlled drug release in drug-eluting stents

With a fundamental understanding of the mechanisms in both therapeutic systems, the concept can now be fully appreciated. As conventional DESs do not maintain drug concentrations within the desired therapeutic window at the target site, it can lead to undesirable and complicated injury-induced effects, as indicated by the graph in figure 2.4. If drug release can be retained in the early days of implantation to promote pro-healing of the arterial wall, and triggered for drug release only during the phase of SMC initiation, it may solve some of these complications encountered. Furthermore, the release will be in the controlled hands of the interventional cardiologist, and be tailored to suit the needs of individual dependent on the condition of the artery itself.

### *2.7.1 Final concept*

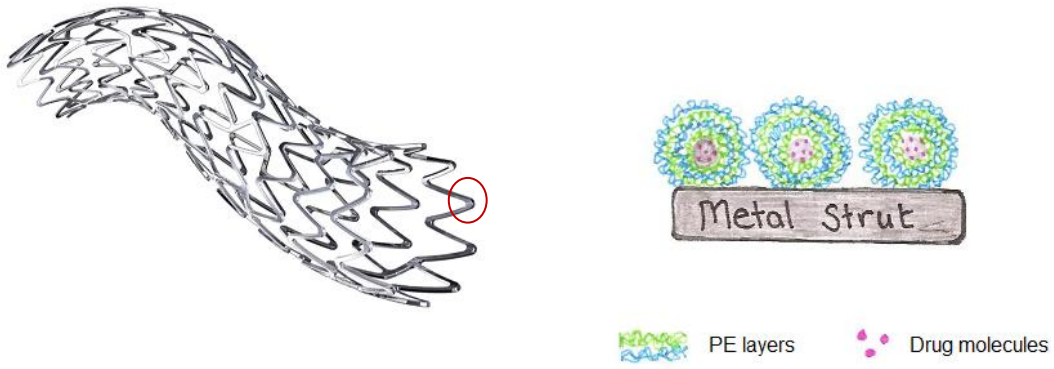


**Figure 2.9: Proposed drug-eluting stent device;** Drug molecules retained securely within PE microcapsules until stimulated by an external triggering source.

# 3 Methodology

## 3.1 Introduction

The experimental procedure for this thesis is to provide a small insight to the field of nanotechnology used as a drug delivery system. Based on our literature, drug-loaded microcapsules have served as a very useful therapeutic technique; a promising tool for the future of local drug delivery. The experiment, therefore, will introduce the concept and feasibility of polylactic acid (PLA) nanoparticles, the multi-layering process and the introduction of AuNP, through the following procedure;

A nanoparticle core of poly(D,L-lactide) is doped with Rhodamine 6G (as a substitute to drug) and will undergo alternate multi-layering of PE PAH and PSS, encapsulating the core. AuNP will be synthesised and incorporated in between the third and fourth layer to improve efficacy. Fluorescent measurements are taken between each consecutive layer, as well as taking SEM imaging.

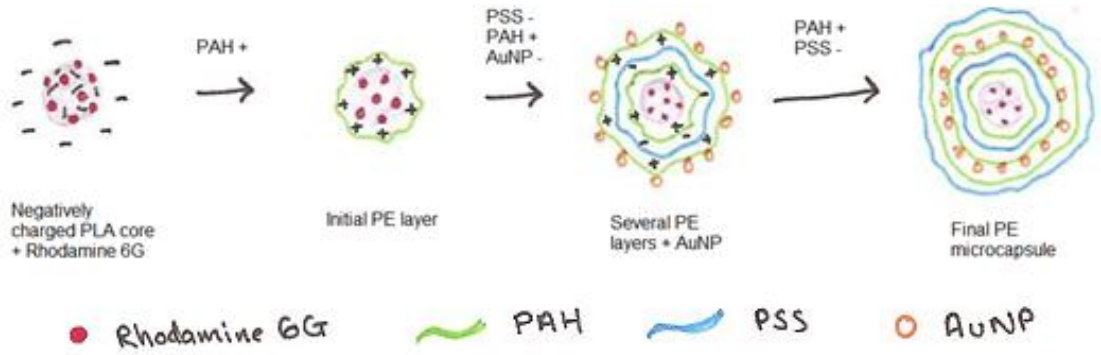


**Figure 3.1:** Schematics of the experimental procedure.

## 3.2 Polylactic Acid Nanoparticles

PLA is an aliphatic, lipophilic, and biodegradable polymer. The constituting monomer, lactic acid, is derived from renewable resources such as corn starch or sugarcane, and is the only degradation product after polymer hydrolysis. PLA and their copolymers is non-toxic within the human body and contain useful mechanical properties, and have been utilised in several medical applications such as tissue

engineering for function restoration of impaired tissues, orthopaedic implants, treatment of scars, and for cosmetic rejuvenation (Rancan *et al.*, 2009).

### 3.3 Dye Incorporation

For simplicity, the PLA core will be doped with a fluorescent dye, as opposed to more ideally a drug commonly employed in DESs. Rhodamine 6G, part of the Rhodamine family, is a lipophilic fluorone dye easily detected using a fluorometer. With an excitation and emission wavelength at 526nm and 555nm respectively, this orange dye will be incorporated into our core. It will allow indication of any damaged or broken microcapsule shells by the release or leakage of Rhodamine 6G. The amount is measured by fluorescence spectroscopy, as well as indicated visually from an observational point of view.

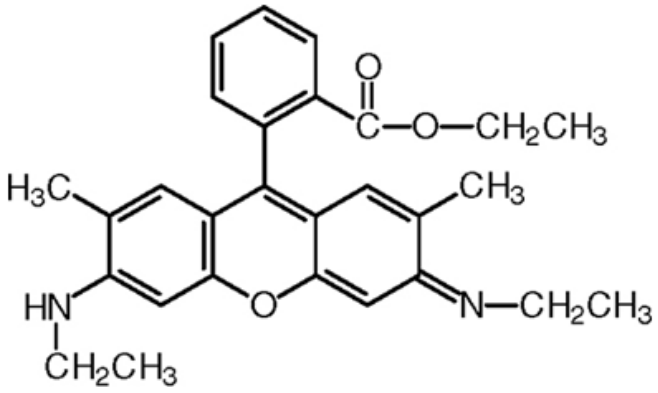


**Figure 3.2:** Chemical structure of Rhodamine 6G.

### 3.4 Polyelectrolytes with Gold Nanoparticles

LbL assembly will be formed by alternatively charged PEs of positively charged PAH and negatively charged PSS, the most commonly used PE pairs as shell components. The first layer is polycation PAH to coat the initial anionic PLA core, and polyanion PSS will subsequently form the second layer. PAH will be used again before introducing negatively charged AuNP. Layering of one or two more PE pairs follows until the required number of layers is achieved.

## 3.5 Preparation of Polylactic Acid Nanoparticles Containing Rhodamine 6G

### *3.5.1 Materials*

Poly(D,L-lactide) (($C_6H_8O_4)_n$, $M_W$ = 18,000-28,000 g/mol, ester terminated, viscosity = 0.25-0.35 dL/g), acetone CHROMASOLV® Plus (($CH_3COCH_3$), $M_W$ = 58.08 g/mol), and Rhodamine 6G (($C_{28}H_{31}N_2O_3Cl$), $M_W$ = 479.01 g/mol,) were purchased from Sigma-Aldrich UK. Distilled water used to prepare the solutions.

### *3.5.2 Equipment*

Kern ABT 120-5DM analytical balance is used to measure material used for the experiment. Jenway model 1000 hotplate/stirrer is used to stir the materials via a magnetic stir bar. Fisher Scientific FB15051 ultrasonic bath is utilised for sonication of solution. Sigma 1-14 microcentrifuge was used to centrifuge the solution.

### *3.5.3 Methods*

The preparation of PLA nanoparticles is based on the method described by Ruggeri *et al.,* (2013) and Lamalle-Bernard *et al.,* (2006). The incorporation of the lipophilic Rhodamine 6G dye is added to the acetone phase, as indicated by Fessi *et al.*, (1992).

5mg of poly(D,L-lactide) is measured and dissolved in 3.33ml of acetone. 0.1mg of Rhodamine 6G is added to this solution and with the addition of a stir bar, the container is placed on a magnetic stirrer for 1 to 2 hours. The mixed solution is added to 8.33mL distilled water (aqueous phase) drop wise under moderate magnetic stirring. The solution is then pipetted into 1mL centrifuge tubes and centrifuged for 5 minutes at 4500 rotations per minute (rpm). The supernatant is removed and kept for the first fluoroscopy measurement. The polymer at the bottom of the tube is individually re-suspended in 0.5mL using distilled water, followed by 1 minute of ultra-sonication (using a water bath) to ensure particles are suspended, and a fluoroscopy measurement of the sample is taken. 10mL is collected from the centrifuge tubes into one glass container, and used for the PE multi-layering step.

## 3.6 Synthesis of Gold Nanoparticles

### *3.6.1 Materials*

Gold (III) chloride trihydrate ($HAuCl_4 \cdot 3H_2O$, $M_W$ = 393.83, 25mMol) was prepared previously within the lab. Trisodium citrate ($(HOC(COONa)(CH_2COONa)_2 \cdot 2H_2O$, $M_W$ = 294.1, ≥ 99%) was purchased from Sigma-Aldrich UK. Distilled water was used to prepare the solutions.

### *3.6.2 Equipment*

Kern ABT 120-5DM analytical balance was used to measure the trisodium citrate. Jenway model 1000 hotplate/stirrer was used to bring the solution to boil whilst under stirring via a magnetic stir bar. Fisher Scientific FB15051 ultrasonic bath was used.

### *3.6.3 Methods*

The synthesis of citrate-stabilised AuNP between 10 and 20nm is employed based on the method explained by Bastus *et al.*, (2011).

0.43g of trisodium citrate is dissolved in a beaker of 50mL distilled water, and placed into an ultrasonic bath for two or three minutes. Subsequently, the beaker is placed on a stirrer and heater, and is covered in foil to prevent evaporation. After 15 minutes of boiling under stirring, 1mL of 25mM $HAuCl_4$ is injected. The initial colourless solution changes from yellow to a bluish grey tint, and then to soft pink within a few seconds. The solution is brought off the boil and left for 30 minutes to cool down, and the colour becomes ruby. The resulting nanoparticles of approximately 13nm is of a concentration ~ $3 \times 10^{12}$ nanoparticles/mL, coated with negatively charged citrate ions and are well suspended in distilled water.

## 3.7 Polyelectrolyte Layer-by-Layer Adsorption with Gold Nanoparticles

### *3.7.1 Materials*

Poly(allylamine hydrochloride) solution (PAH, 2g/L, 6mMol NaCl), and poly(styrene sulfonate, sodium salt) (PSS, 2g/L, 6mMol NaCl) were synthesised previously within the lab. Concentration is diluted by half using a 1:1 ratio of distilled water, to 1g/L. Citrate-stabilised AuNP were synthesised as mentioned.

### *3.7.2 Equipment*

Jenway model 1000 hotplate/stirrer and magnetic stir bar, Fisher Scientific FB15051 ultrasonic bath and Sigma 1-14 microcentrifuge are utilised to form the multi-layering.

### *3.7.3 Methods*

The suspended PLA nanoparticles in approximately 5mL of distilled water are now subjected to the first PE layer in a 1:1 volume ratio. 5mL of PAH of concentration 1g/L is added to the solution, and is placed on the stirrer for 2 hours, to allow interaction between the PLA nanoparticles and PAH solution. Following this, the solution is centrifuged for ten minutes at 10000 rpm. The supernatant is removed and kept for fluoroscopy measurement to determine if the retained dye has leaked. The particles are suspended again in 0.5mL each, and after sonication in the ultrasonic bath for a couple of seconds, the solution is collected for the second PE layer. 5mL of PSS of 1g/L concentration is added and the solution is mixed for 2 hours. After centrifuging using the same parameters, particles are re-suspended again in 0.5mL distilled water, taking fluoroscopy measurements of the supernatant. PAH is used to form the third layer, using the same technique mentioned. Once the PLA nanoparticles undergo three successive layers, 2mL of negatively charged AuNP solution previously synthesised is added. The above layering process is then repeated for the final two layers, starting with PAH.

**PLA + DYE / PAH / PSS / PAH / AuNP / PAH / PSS**

## 3.8 Fluorescence Spectroscopy Analysis

### *3.8.1 Equipment*

A Fluorometer Jasco V660 Spectrophotometer is used to obtain the absorption spectra of the remnants of Rhodamine 6G solution, using Spectra Manager computer programme to process the data. For the emission spectra, a FluoroLog® 3 Spectrophotometer is used, with the spectrum obtained using FluorEsscence V3.5 computer software, and OriginPro 9 to convert the data into an excel format.

**Figure 3.3:** *Left:* Jasco V660 Fluorometer and computer software for absorption analysis. *Right:* FluoroLog 3 spectrometer for emission analysis.

### *3.8.1 Methods*

Fluoroscopy measurements of our sample and the eliminating supernatant are taken prior to the first PE layering, to determine the percentage of Rhodamine 6G retained with the PLA core. The absorption of the solution is measured between wavelengths 300nm to 800nm using plastic cuvettes, and placed in the Jasco V660 spectrometer. The baseline for the supernatant at this point is only acetone and distilled water, using the same ratio used to dissolve the poly(D,L-lactide). For the sample, the baseline is simply distilled water. Once the peak absorbance is obtained, this determines the parameters used for the emission spectrum in the FluoroLog® 3 spectrometer. For Rhodamine 6G, this was typically an excitation peak of 520nm, with a range of 530nm to 800nm. The same procedure is used to measure the absorbance and emission of only the supernatant after each consecutive layer, using distilled water as the baseline. This indicated whether the dye was still retained.

## 3.9 Scanning Electron Microscope Analysis

### *3.9.1 Equipment*

A Hitachi TM-1000 tabletop Scanning Electron Microscope (SEM) is an imaging platform used to analyse the nanoparticles and the PE microcapsules.

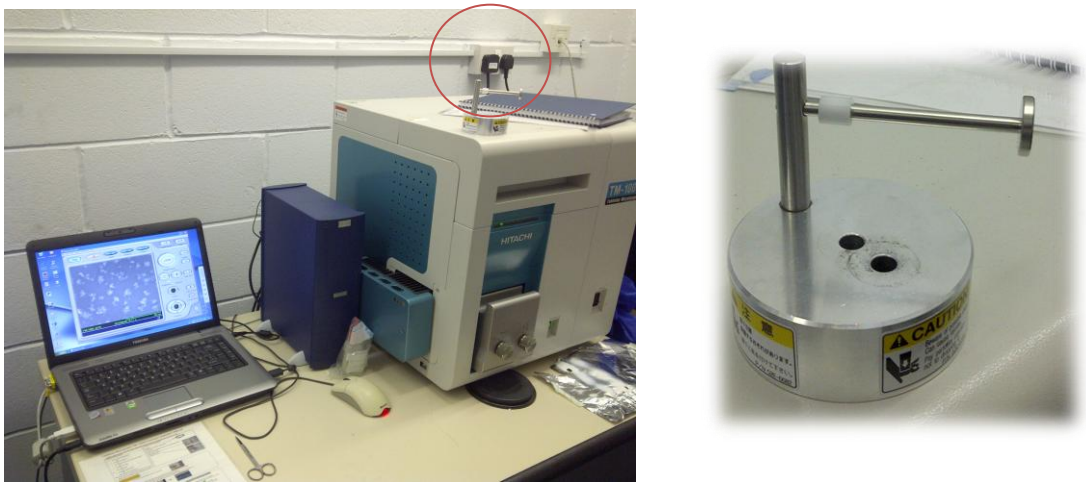


**Figure 3.4:** *Left*: SEM system used to analyse the samples for the experiments. *Right*: Specimen holder placed into the machine for SEM analysis

### *3.9.2 Methods*

Prior to all SEM imaging, the samples requires being dry. As most of the samples are suspended in distilled water, a drop of the sample is placed onto a small glass cover slide, and left overnight to dry out. The first SEM image taken is of the initial PLA nanoparticles prior to PE multi-layering. Subsequently, images are taken of the AuNP solution, the multilayered microcapsule at the AuNP layer stage (i.e. PLA with dye/PAH/PSS/PAH/AuNP), and the final PE microcapsule. Images are taken from a range of magnifications from x200 to x10000.

# 4 Results and Discussion

## 4.1 Introduction

The experimental section introduced the concept of PE microcapsules based on a PLA nanoparticle core. This is a relatively new technique serving in many useful biomedical applications, with our own future aim to implement this onto a stent. The purpose of using a dye was to simplify matters, and estimate the amount of dye retained after the procedure. Although the methodology is thought to have been straight forward, it wasn't without its complications. The results are gathered and these will be discussed further, alongside suggestions to some of the difficulties encountered.

## 4.2 Polylactic Acid Nanoparticles

The initial step of the experiment is to formulate a PLA core to which the PE layers are subjected to. The poly(D,L-lactide) instantly dissolved in the organic solvent acetone, and the addition of a small quantity of Rhodamine 6G turned the solution into bright orange. The solution is mixed for 1 or 2 hours and covered in foil to preserve the dye. After thorough mixing, this acetone phase is added drop wise into distilled water. The solution becomes a cloudy orange, or opalescent if no dye is incorporated. This transfer resulted in the formation of PLA nanospheres.

**Figure 4.1:** Opalescent PLA nanoparticles without dye suspended in water (against green background).

This is what is expected, according to Fessi *et al.,* (1992), since the acetone rapidly diffuses out from the emulsion droplets and towards the aqueous phase, drastically reducing the size into a nano-size order, as mentioned by Orozco *et al.,(* 2010) and Murakami *et al.,* (1999). This solvent-diffusion method solidifies the droplets to form polymeric nanoparticles. If the aqueous phase is not subjected to moderate stirring during the addition of the acetone and PLA solution, it results in a thin clear film over the top, presumably the aggregation of the PLA. This also occurred if the acetone phase is not added in a drop wise manner. This was one of the difficulties often observed during this experiment step, and took multiple repetitions to rectify.

The solvent used in this experiment is acetone, an organic lower alcohol capable of dissolving the PLA substance, and is miscible with our non-solvent distilled water. It is recommended that for a more stable suspension of nanoparticles, that a surfactant be introduced to the aqueous phase (Fessi *et al.,* 1992). This is more likely useful when a drug ingredient is incorporated, to ensure all drug molecules are retained. If the drug is a lipophilic active ingredient such as indomethacin and paclitaxel, the addition is employed in the acetone phase, where up to 80% of the initial amount is incorporated into the nanoparticles. For hydrophilic drug ingredients like penicillin, these are either introduced to the aqueous phase, or subsequently during the PLA suspension, resulting in ~ 30 – 50% drug incorporation.

Our solvents are then removed via centrifugation using a low speed of 5000 rpm for 5 minutes. This resulted in the soft polymer particles accumulating at the base of the centrifuge tube. When the supernatant is eliminated, the particles are easily suspended in distilled water. However, if the speed of the centrifugation is too high, the polymer particles aggregate together which cannot be separated, even after sonication. Alternatively, the solvents may be removed under reduced pressure without heating to a desired volume using a water pump vacuum, and the concentrated suspension filtered using a glass frit. This may be an easier alternative to ensure no PLA nanoparticles are lost. The supernatant and our sample are measured using absorbance and fluoroscopy measurements to determine the percent of dye within the PLA nanoparticles.

### *4.2.1 Scanning electron microscope analysis*

A sample of the suspended PLA nanoparticles were taken and dried on a glass cover slip. The following day, this was placed into the SEM machine for our first analysis.

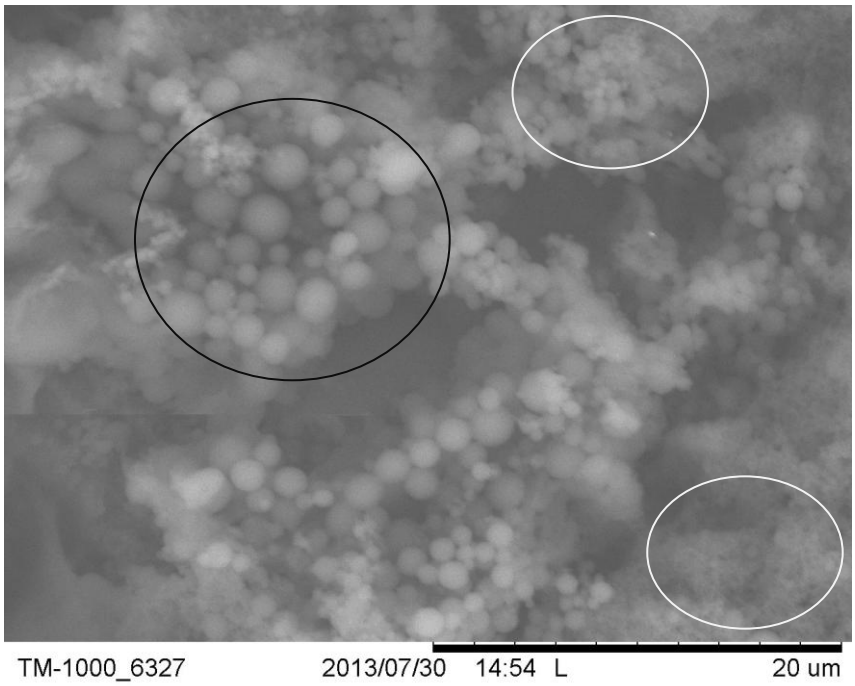


**Figure 4.2:** SEM image of PLA nanoparticles under 4000x magnification, without Rhodamine 6G dye (these particles were not used in the final product).

The SEM visibly shows PLA nanospheres. The sizes seem to vary but this may be due to the drop being unevenly distributed over the cover slip. The larger sizes (circled in black) have roughly an estimated average size 600nm. The smaller clusters of nanoparticles (circled in white) are of a much lesser size, roughly around 300nm. For a more accurate depiction of the size distribution, quasi-elastic light scattering could have been used, which determines the size of small particles in suspension. This was used in the Lamelle-Bernard *et al.*, (2006) methods, for their formation of anionic PLA nanoparticles using poly(D,L-lactic acid), determining their size of 220 ± 19nm. Furthermore, the Fessi *et al.*, (1992) states that using the method employed in our methods prepares spherical particles of the matrix type of a size less than 500nm (between 180 – 280nm), hence the sizes of our PLA nanoparticles are questionable.

### *4.2.2 Spectroscopy measurement*

The supernatant is removed and tested for the first measurement. Thereafter, supernatant is eliminated from the procedure.

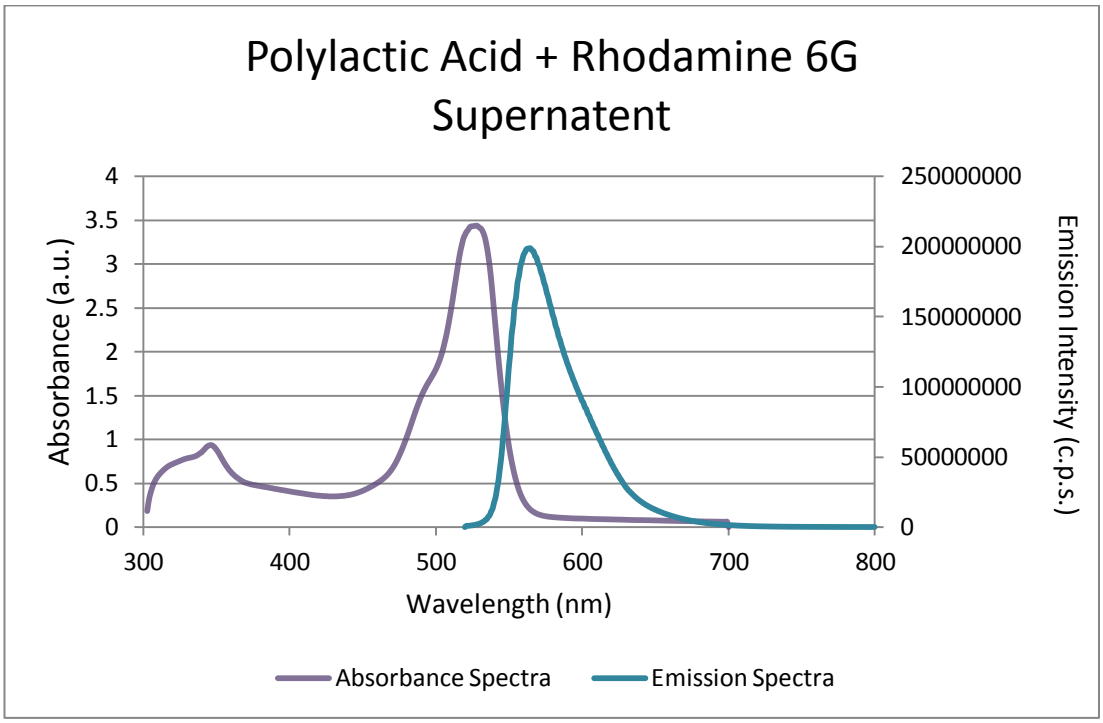


**Figure 4.3:** Measured absorbance and emission spectra of eliminated supernatant prior to first PE layering.

The graph shows a typical optical absorption measurement of Rhodamine 6G. The wavelength range used is from 300nm to 700nm, with an absorbance peak measured at 529nm. The absorbance measures the intensity of the colour, with higher absorbance deeming more concentrated, and for the supernatant this measured at an absorbance of 3.44 at 529nm. At wavelengths 350nm and less, the signal begins to fluctuate slightly due to noise. The fluorescence emission spectrum of Rhodamine 6G is measured from 530nm to 800nm. The emission wavelength for the peak is at 563nm, with emission intensity of 1.99 $x10^8$. Therefore, there is 34nm between the two peaks; a shift phenomenon known as Stokes shift. This also contributes to a small overlap between the higher wavelength end of the absorption spectrum and lower wavelength end of the emission spectrum.

To measure the remaining dye within our solution, a sample is taken from the suspended particles in distilled water, and the same parameters were implemented.

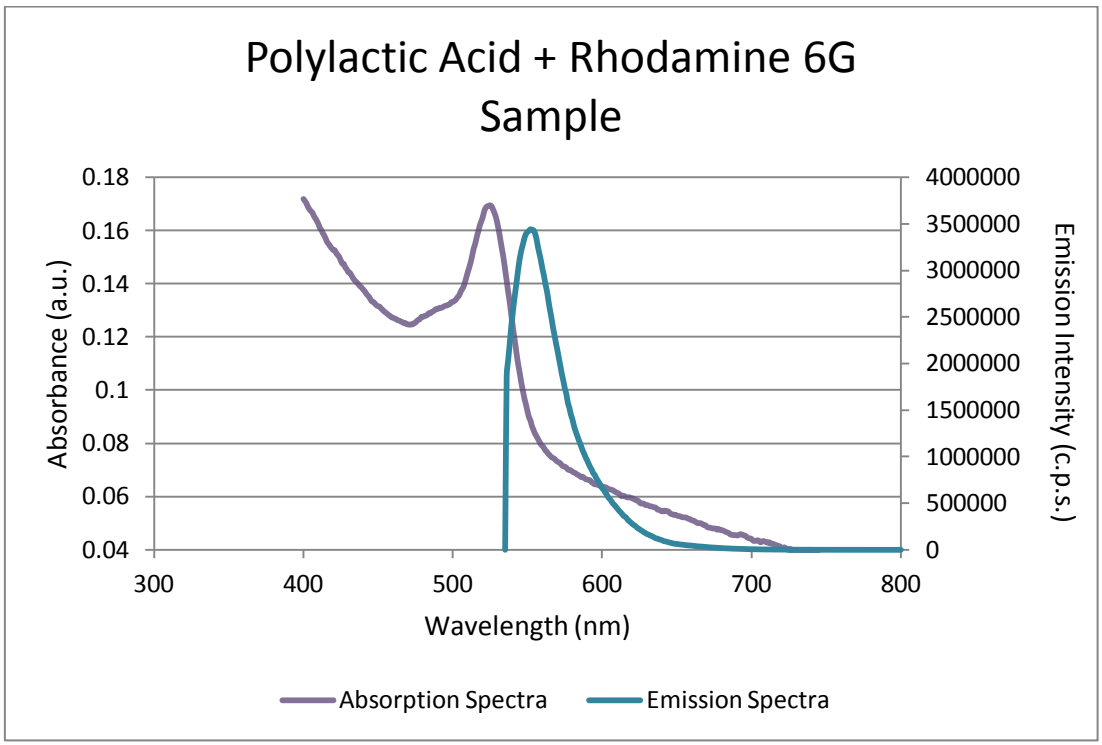


**Figure 4.4:** Measured absorbance and emission spectra of sample prior to first PE layering.

It is noticeable that both graphs show the same shape, with the exception of another absorbance peak at the lower wavelength end. For Rhodamine 6G, the absorbance peak occurred at 525nm, with an absorbance of 0.17; a decrease in wavelength of 4nm. The second rising peak is the detection of another component within the sample, which are our PLA particles. The amount of dye retained can be estimated to be almost a 1:20 ratio. For the emission, the peak is measured at 551nm with an intensity of 3.45 $x10^6$; another shift to a lower wavelength. Between the two peaks, there is 26nm, a much lesser shift than in the supernatant. This results in a spectral overlap much larger than that observed in the supernatant. It is also noted that the width of the peaks are much narrower than that of the supernatant.

### *4.2.3 Basics of optical absorption and emission*

To understand the rationale of the absorption and emission spectrum, some fundamental principles need to be understood. Rhodamine 6G is a fluorophore, a fluorescent chemical which re-emits light upon excitation. For this, they exhibit unique characteristic spectra for absorption and emission, detailing the relative intensity of fluorescence. The absorption measures the wavelengths to which the material absorbs light photons in order to move electrons into an excited state due to the energy gain. This state only lasts in the region of a couple of nanoseconds. The absorbance spectrum, to a certain approximation, is equivalent to the fluorescence excitation spectrum. It does not attain units as it is a logarithmic ratio of the amount of light falling upon the material to the amount transmitted through the material.


**Figure 4.5:** Wavelengths of light visible to the human eye [8].

For the fluorescence emission, the intensity is quantitatively dependent on the same parameters as the absorbance. The material returns back to the stable ground state by emitting a photon, and there is a loss of energy from the system in the form of vibration energy, or possibly rotational energy. The emitted light wavelength is typically longer than that of the absorbed light; therefore it is of a lower energy.

Stokes shift is the wavelength difference between the peak maximum of the absorption and emission spectra. If the emitted photon contains less energy than the absorbed photon, the energy difference accounts for the Stokes shift. This results in the emission spectrum to be shifted to longer wavelengths than the absorption spectrum. The greater the shift, as observed in the supernatant, the easier it is to distinguish the light produced by the emission from the light used to excite the particles. For the sample, the shift is much smaller with a large overlap, and suggests that the parameters implemented were not in sync with the absorption maximum.

Spectroscopy measurements determined that as much as 95% of Rhodamine 6G was eliminated at this stage, leaving only ~5% retained within the PLA nanoparticles.

## 4.3 Synthesis of Gold Nanoparticles

For the synthesis of citrate-stabilised AuNP, the method simply followed the procedure in Bastus *et al.*, (2011). During the initial experiment, no colour change was observed. After consideration, it was realised that the concentration of gold (III) chloride trihydrate was incorrect; 2.5mMol was used instead of 25mMol. Once this was rectified, the colour change was imminent.

**Figure 4.6:** Ruby colour indicating success of the AuNP coated in citrate ions of size 10 – 15nm.

The ruby colour appears due to the plasmonic optical properties of the AuNP. As white light interacts with the particles, certain colours are absorbed, which are blue and green this case. Red light is transmitted through the material, which is the colour observed in this procedure.

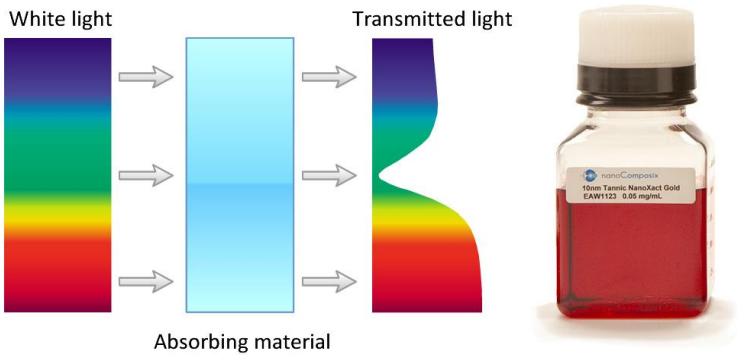


**Figure 4.7:** Schematic of white light interaction with small AuNP, resulting in the transmission of red light [8].

### *4.3.1 Absorption spectra*

A cuvette of AuNP solution is placed into the fluorometer for absorption analysis.

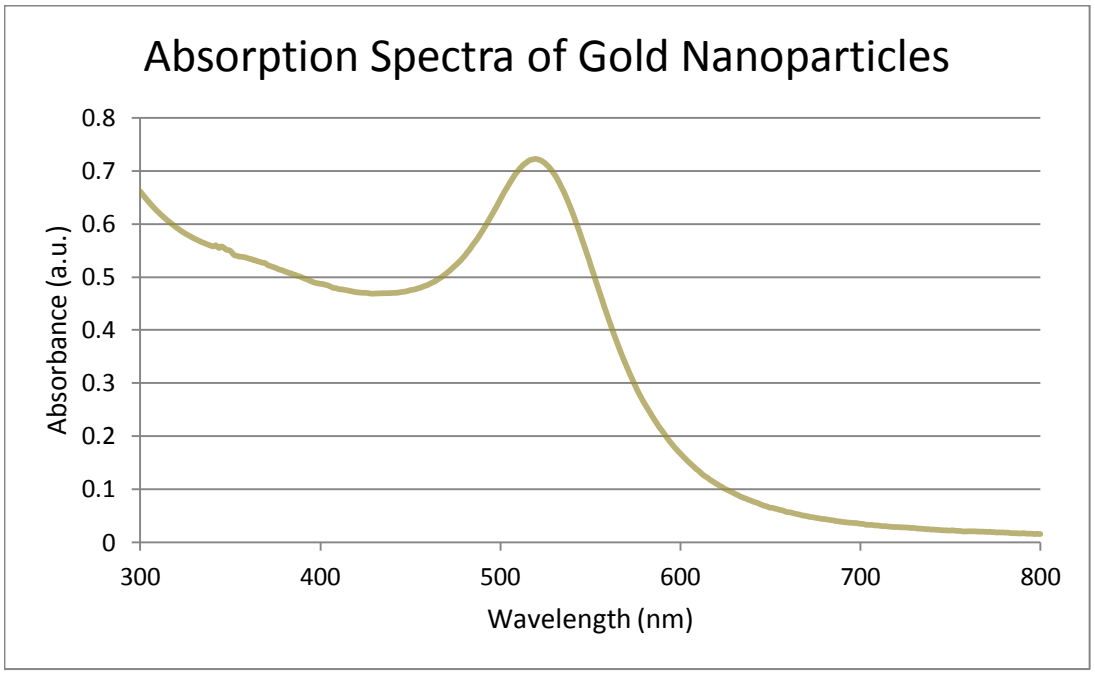


**Figure 4.8:** Absorption spectra of AuNP spanning over wavelengths 300nm to 800nm.

The absorption depicts a true spectral shape for colloidal gold nanoparticles. The maximum peak occurs at 520nm with an absorbance of 0.723. The peak indicates that the nanoparticles are between ~ 10 to 15nm in size. Figure 4.9 indicates that at this peak, green and blue photons are absorbed by the nanoparticles, hence only observing the transmitted colour, opposite to that absorbed.

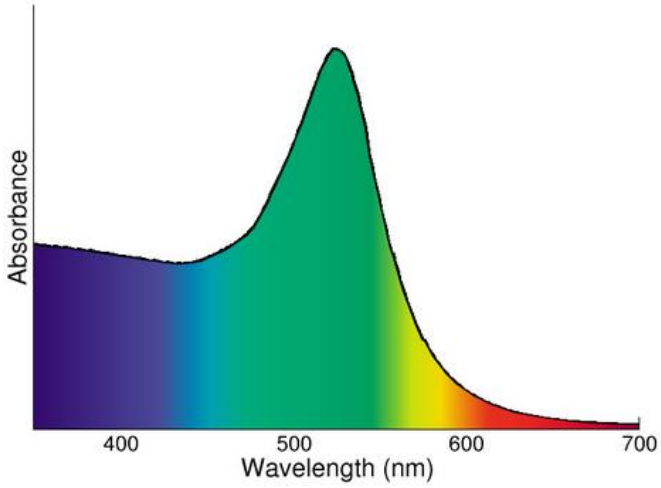


**Figure 4.9:** Absorption spectrum of ~ 13nm AuNP. Inset depicts colours that are being absorbed [8].

### *4.3.2 Scanning electron microscope analysis*

A drop of the synthesised AuNP solution is placed into the SEM for analysis.

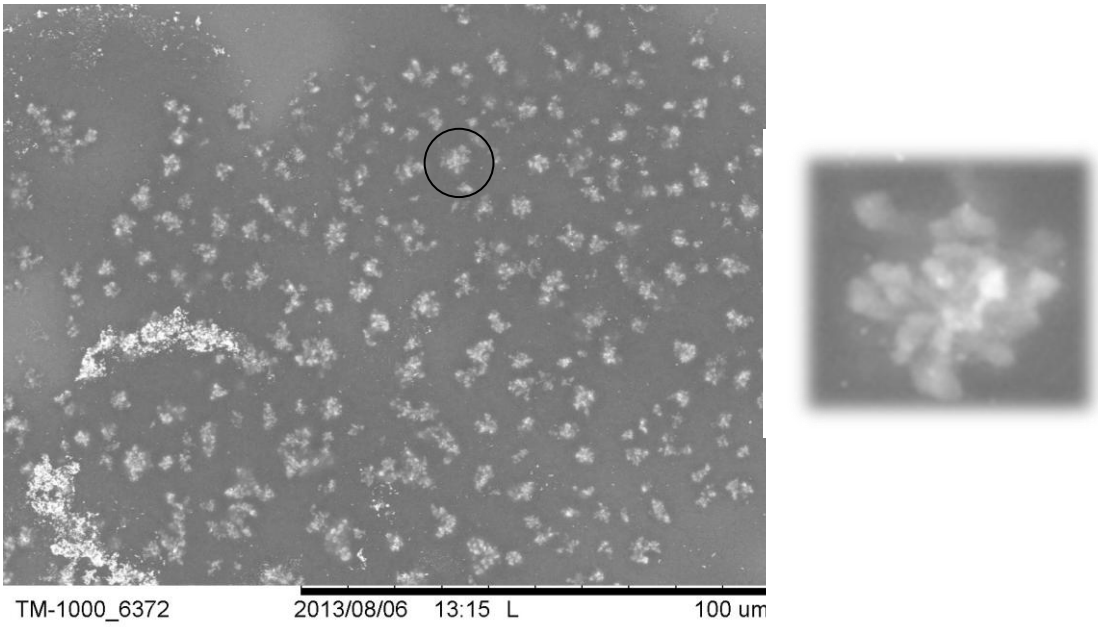


**Figure 4.10:** *Left:* SEM analysis of AuNP clusters at 1000x magnification. *Right:* zoomed in inset of an AuNP cluster at 5000x magnification.

As the sample dries, the nanoparticles begin to aggregate together, as shown in the many clusters observed in the SEM image. The zoomed image to the right shows a cluster with a solid-like centre of many AuNP. Of the larger clusters, sizes seemed to vary between 2µm and 10µm.

The synthesis was easily prepared using the reducing agent sodium citrate, resulting in very stable AuNP. The size of nanoparticles can be modified by varying the concentration of the sodium citrate, and these citrate ions can be replaced easy by readily attaching molecules of biological interest such as DNA and antibodies (Huang *et al.*, 2007).

### *4.3.3 Gold nanoparticle properties*

Compared with other nanostructures, noble metal nanoparticles possess great potential for biomedical application. They attain low toxicity, tuneable optical properties, and their shape, size, assembly, and structure can be synthetically controlled. Most promising of the noble metals is the AuNP, and optical properties such as light absorption, emission (luminescence), and Rayleigh scattering (light scattering at same frequency as incoming light) are all strongly enhanced. Of this, their application has gained keen interest in molecular-specific cancer detection and therapy, as explained by Huang *et al.,* (2007). For AuNP, they can be bioconjugated with anti-epidermal growth factor receptor (EGFR) antibodies, which can be visualised by monochromatic light illumination, used to immunotarget specific cancer biomarkers. Additionally, as mentioned by the same author, studies have demonstrated that using 40nm AuNP conjugated with anti-EGFR antibodies can be used to target cancerous cells that specifically overexpress EGFR on the cell surface.

Furthermore, AuNP can be used solely as a drug carrier for targeted delivery of chemotherapeutics. Several *in vivo* investigations with tumours implanted within various locations in mice are mentioned by Dykman and Khlebtsov (2012). These have included paclitaxel, doxorubicin, methotrexate, and tamoxifen, with most studies noting high effectiveness of using these preparations.

For our particular application, the AuNP is incorporated in between the PE layers to act as an ultrasonic switch to release the drug. AuNP, as well as silver nanoparticles, attain sensitivity which absorbs ultrasonic energy. Pavlov *et al.,* (2011) investigated the properties of PE microcapsule rupturing under ultrasonic triggering with the presence of AuNP. It was evident that AuNP within the polymeric shell assisted in fragmentation at a lower frequency of 850 kHz. Although the majority of AuNP are lost to the supernatant during centrifugation, the remaining AuNP possess key characteristics. Their presence results in the PE microcapsule to become heavier, thus the oscillating movement and vibration becomes easier; a factor influencing the rupturing. Furthermore, the absorption of ultrasound energy causes the microcapsules to heat. As AuNP retain much of the thermal energy, it prevents the rapid heating of the polymers, and can limit the release of the encapsulated load (Pavlov *et al.,* 2011).

## 4.4 Polyelectrolyte Microcapsules

Once the PLA nanoparticles and AuNP were synthesised, the PE multilayering process began. The initial suspended PLA nanoparticles with Rhodamine 6G were coated instantly to retain as much of the remaining dye. The first layer is PAH, to coat the anionic PLA, and a 1:1 volume ratio of 1g/L PAH solution was used. 5mL of suspended PLA nanoparticles and 5mL of PAH were left under moderate stirring for 2 hours, to ensure particle interaction. Visibly, small white particles are seen suspended in solution. This solution is then centrifuged to remove the excess PAH and distilled water. The centrifuge rate at 10000 rpm for 10 minutes resulted in the particles accumulating at the base and along one side of the centrifuge tube, but this is vaguely seen. Once the supernatant is carefully removed, the particles are resuspended in a total of 5mL distilled water, with 5mL of PSS and left to stir further for 2 hours. Spectroscopy measurements were taken for this supernatant, but from an observational view, the vague discolouration indicated that more dye had leaked. The process is repeated, until three alternative layers were achieved. The centrifuge rate was increased to 14000 rpm since the particles were not clearly visible after the first centrifugation cycle. It became evident that after each consecutive layering, the PE microcapsules became more dilute, and more were lost to the supernatant.

Following the initial three layers, 2mL of our AuNP solution is introduced to the 5mL of resuspended particles. The solution became a light ruby colour, and this is left overnight on the stirrer. One of the problems observed the next day, is that the AuNP had aggregated onto the magnetic stirrer and onto the side of the glass container. The procedure was repeated from the start, and all equipment was ensured to be thoroughly cleaned with ethanol between each new layer. It was possible that some PE particles had remained onto the glass side and stirrer and this lead the gold to aggregate. After centrifugation, a sample is taken for SEM analysis and the final two layers are applied using same volume ratio. It was also noticed that by this point, no particles were actually visible by the eye, except from the AuNP colour, which lead to questioning of the effectiveness of the PE layering procedure. By the end of the layering procedure, the solution was almost clear, as to say that no particles had remained. A final sample is taken for SEM analysis to see if this was the case.

### *4.4.1 Spectroscopy measurement*

The eliminated supernatant was measured for its absorbance, to indicated Rhodamine 6G leakage.

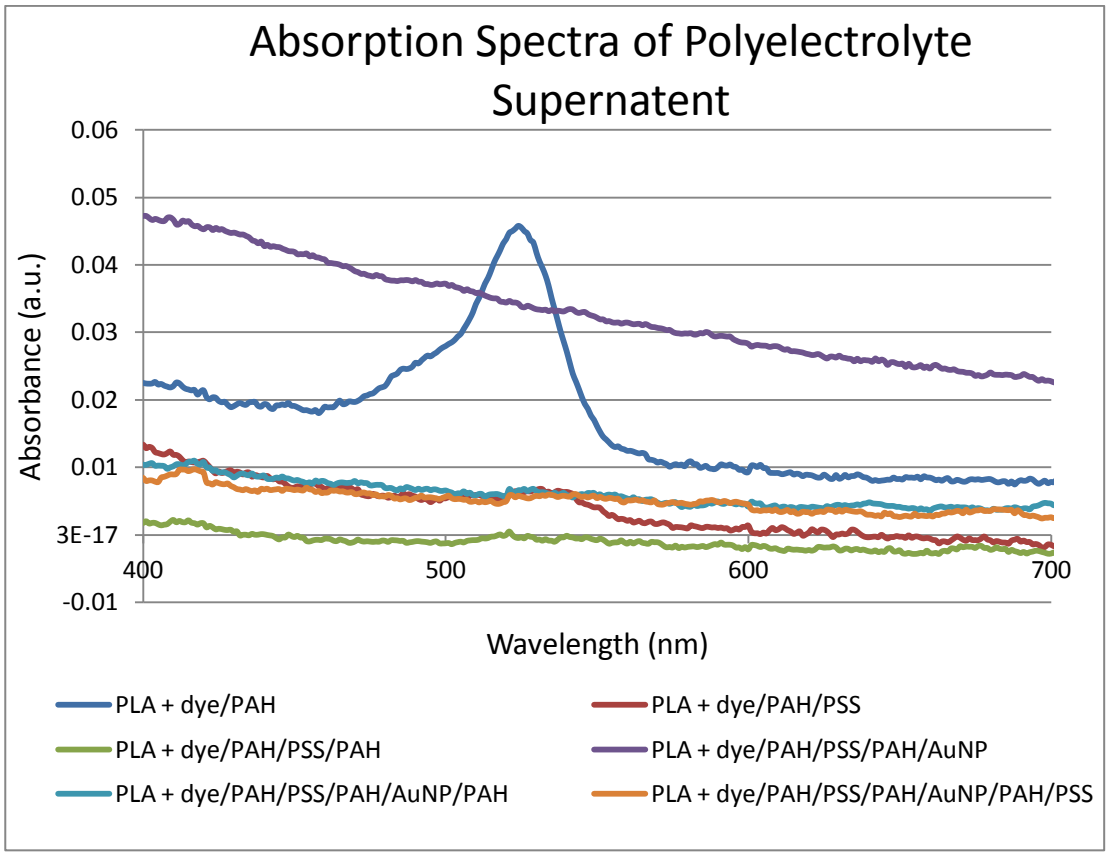


**Figure 4.11:** Absorption spectra of the supernatant after each consecutive PE layer, from wavelength range of 400 to 700nm.

The parameters are conformed suitable to Rhodamine 6G, from a wavelength range of 400nm to 700nm. After the initial PAH layer, the supernatant revealed to have an absorbance peak at 524nm with an absorbance of 0.046. There is a shift of 4nm to a shorter wavelength between this peak and the peak absorbance of the PLA nanoparticles with dye. This is known as a blue shift. Approximately a quarter of the remaining Rhodamine 6G dye is lost at this point. For the following layers, very little dye is determined. The solutions are very dilute, and the absorbance is giving nothing measureable. For the supernatant measurement of the layer after AuNP (i.e. purple), no dye is detected but the absorbance slope is raised, and therefore it is detecting the presence of another component (AuNP).

After the absorbance, each supernatant is measured for its emission (note that some data are multiplied to give a clearer depiction of the shape).

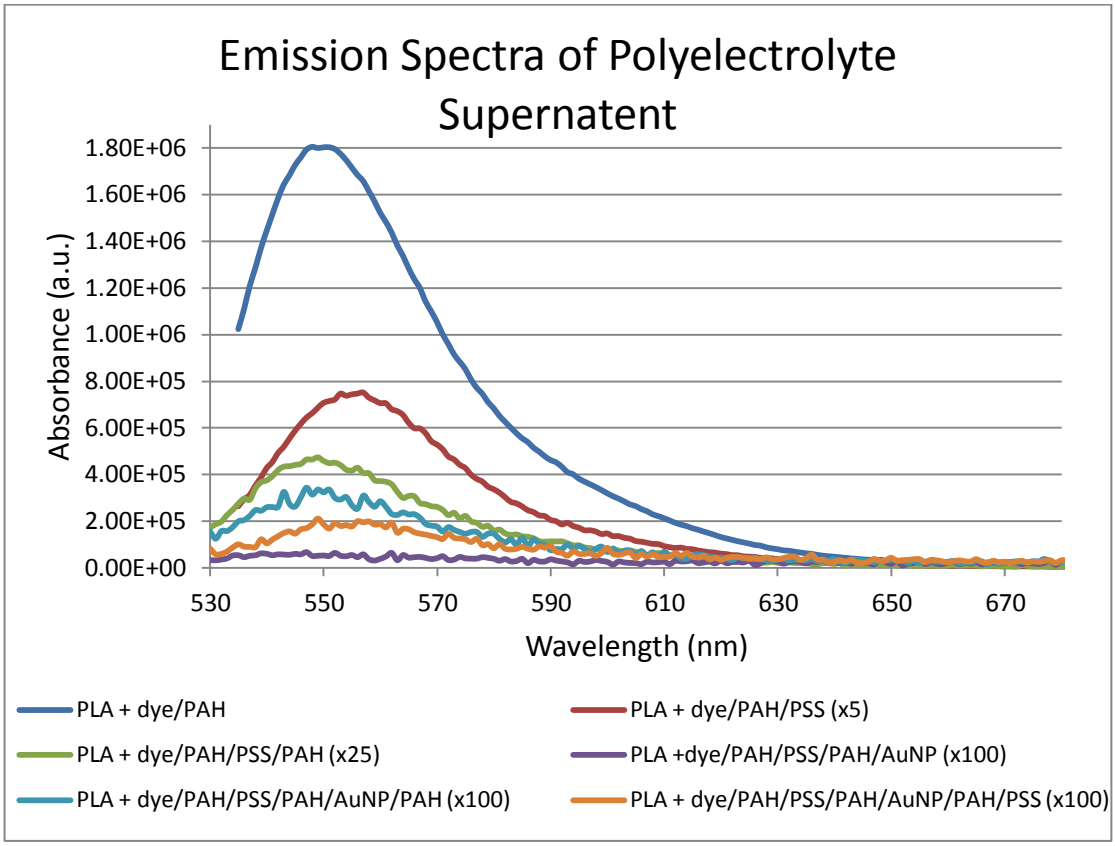


**Figure 4.12:** Emission spectra of supernatant after each consecutive PE layer, from wavelength range of 530nm to 680nm, with excitation peak of ~520nm.

The peak maximum of each emission is much more easily observed compared to the absorbance. For the initial PE layer, the peak maximum occurs at 548nm, a blue shift of 15nm compared to the first supernatant. The maximum peak of the second layer indicates a red shift to a longer wavelength of 557nm. For the third layer, the maximum peak shifts back to 549nm; blue shift. These occur due to the alternatively charged species between the positive PAH and the negative PSS.

When AuNP are incorporated, the peak shifts slightly to a shorter wavelength of 547nm and the same maximum is observed in the following PAH layer. For the final PE layer, the maximum occurred at 549nm. Since almost no shifts are determined in these final layering stages, this suggests that there were no charged PE species remaining in the solution.

It is evident that during the first PE layering, and in the following successive layers, small amounts of Rhodamine 6G is detected. By the end of the procedure, either a little dye is retained within the PLA core, or most probable, that all of the dye has been eliminated in the previous stages. It was clear that after the AuNP layering stage, the particles that were once easily observed in the early stages of suspension, were not clearly visible. This contradicts almost all studies which indicate that increasing the number of PE pairs provide stability within the capsule, and some suggest that for optimum stability, the minimum number of PE layers is ten (Kolesnikova *et al.,* 2008).

### *4.4.2 Scanning electron microscope analysis*

SEM imaging is used to analyse the PE microcapsules after the AuNP layer. Particles of the microcapsules are observed, but not as a complete capsule entity.

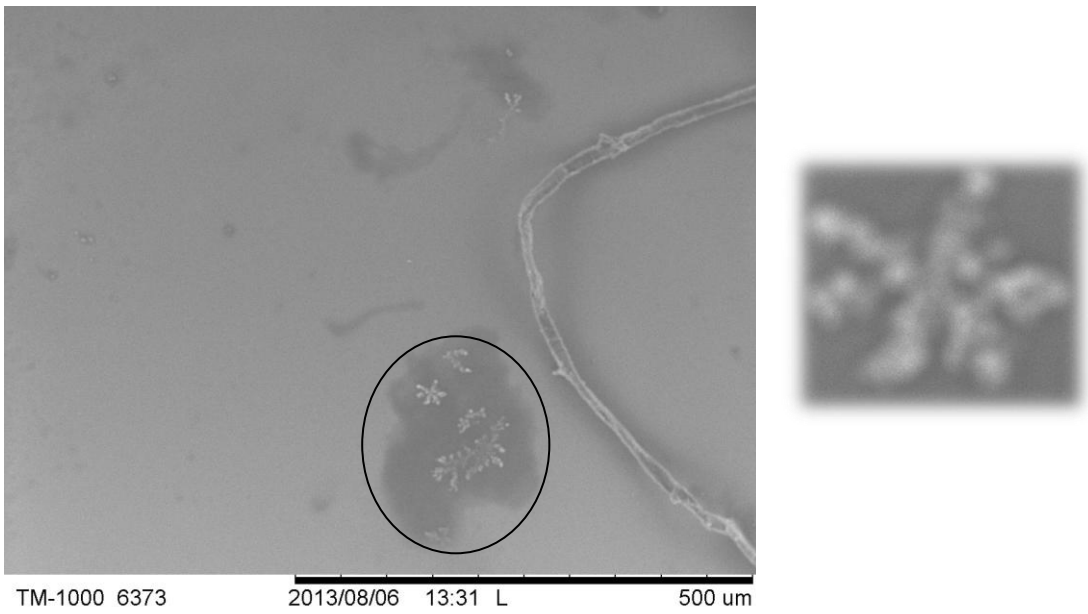


**Figure 4.13:** *Left:* SEM analysis of PE microcapsule particles (circled) with AuNP as the outermost layer, at x200 magnification.
*Right:* zoomed in inset at x12000 magnification

SEM analysis taken after completion of the procedure came up blank, and nothing was observed apart from sparse and random individual particles that could not be clarified as PE microcapsules, and therefore the images were omitted.

### *4.4.3 Efficacy of polyelectrolyte microcapsules*

Unlike our experiment, when the correct conditions and parameters are implemented, PE microcapsules can be used effectively as a carrier for many materials including biomolecules, drugs and cells. Mak *et al.,* (2008) studied the stability and the encapsulation efficacy of PE microcapsules by varying the temperature and the types of PEs used. Polycations PEI and poly(diallyldimethylammonium chloride) (PDA), and polyanions DS, and polyacrylic acid (PAA) were investigated alongside PAH and PSS.

One of the notable aspects discovered is that PEs with strong ionic strength and high charge density contributed to more stable and formed capsules, whereas weaker PE pairs (such as PAH/PAA) aggregated instantly during the second PE layering. Although PAH is a relatively weak PE compared to the other polycations, it is counterbalanced by a strong anionic PE, i.e. PSS.

To determine the encapsulation efficacy, the amount of biomolecules retained within the microcapsules is compared to the initial amount, and factors influencing this efficacy are the molecular size of the encapsulating material and the PE paring used for microcapsule fabrication. With reference to Mak *et al.*, (2008), PAH was the polycation with the highest encapsulation efficacy, and this was strengthened with the pairing of PSS.

Finally, the stability of the PE microcapsules of various pairings was tested against temperatures varying from 65°C to 95°C; necessary as certain biochemical reactions occurs at high temperatures. Pairings with PEI proved to be the most unstable, whereas PAH/DS microcapsules left behind fragmented and broken capsules due to the weakening of the electrostatic interactions between the PEs. In contrast, 75% of the PAH/PSS microcapsules remained stable with perfect spherical shape, with their contents retained within the capsules.

Therefore it was concluded that PE pairing of PAH/PSS (with PSS as the outermost layer) fabricated microcapsules with good balance of colloidal and temperature stability with high encapsulation efficacy (Mak *et al.*, 2008).

# 5 Implementation and Future Work

## 5.1 Introduction

The experimental aspect of this project was to simply introduce PE microcapsules as a tailored and controlled technique for drug delivery. In summary, the synthesis of PLA nanoparticles with initial retention of Rhodamine 6G was achieved, alongside synthesis of AuNP in suspension, and this can be easily replicated following the methods. The same cannot be said for the fabrication of PE microcapsules with PAH and PSS. The continuous loss of particles at each following stage requires revision of the initial methodology due to its lack of efficacy.

However, these experiments were only a small part of a much larger vision. As intended, the aim is to incorporate drug-loaded PE microcapsules onto stents to trigger drug release at key time intervals and inhibit the pervasive ISR. The following sections are suggested future work to take the idea forward.

## 5.2 Drug-Loaded Polyelectrolyte Microcapsules onto Stent

One of the most challenging situations currently faced in the field of therapeutics is the delivery of water-insoluble organic drugs, which represent a large proportion of anti-inflammatory drugs and chemotherapeutics. Drug bioavailability is greatly reduced when these drugs are injected systemically due to their high affinity for lipid cell membranes and spontaneous aggregation within the bloodstream (Boudou *et al.*, 2012). Hence, the recent introduction of nano- and micro-carriers aims to reduce these toxicity profiles and optimise therapeutic efficacy.

Currently, one of the main progressions in utilising drug-loaded PE microcapsules is in the application of chemotherapy, for the treatment of solid tumours. At present, the irregular vasculature and blood flow have proved too difficult for conventional direct drug delivery, which is also hindered by the drug hydrophobicity properties. One of the limitations of current chemotherapy techniques is the lack of specificity towards the neoplastic cancerous tissues, and systemic injections cause significant

damage to healthy tissues. This results in serious side effects including alopecia, anaemia, nausea and pain, to more systemic toxicity within the heart, liver and kidneys. Therefore, smart drug delivery systems are imperative in these situations, and a great deal of research has been in progress.

Boudou *et al.,* (2012) successfully loaded paclitaxel in the hydrophobic region of the shell, as the drug cannot be encapsulated within the hydrophilic core. The dose of drug within each microcapsule can be varied by modifying the number of PE layers, the concentration of the initial dose of paclitaxel and the polycation used. A biodegradable template core is used, which is later removed by a mild process to leave behind a hollow microcapsule. Furthermore, the same group demonstrated the selective entrapment of paclitaxel on a flat surface plane, an alternative to spherical microcapsules.

For our own implementation, the intention is to synthesise paclitaxel-loaded PE microcapsules similar to that mentioned by Boudou *et al.,* (2012). Once this is achieved, techniques need to be designed on how the microcapsules are attached to the stent. A possible suggestion is to utilise the electrophoretic deposition (EPD) approach, where colloidal particles suspended in solution migrate and are deposited onto an electrode via an electrical field, and has been used to coat metal fabricated products. Therefore, EPD can be possibly used to coat uniformly and tightly PE microcapsules over the stent surface. Other techniques may need to be designed due to its novel application, which is something to investigate in the future. It may be more feasible to achieve layering of drug-loaded PE onto a planer, flat surface, as achieved by Boudou *et al.,* (2012), and have multiple PE layers coating the stent with paclitaxel, or any other hydrophobic drug, in between the layers. This will cover a larger surface area and able incorporate more drug molecules.


**Figure 5.1:** *Left:* Paclitaxel-loaded PE layers on flat surface.
*Right:* Paclitaxel-loaded PE microcapsules before and after core removal.

## 5.3 Ultrasonic Triggered Drug Release

The pivotal component of our stent design is the novel drug release mechanism from an external ultrasonic source; remote controlling the release in a desirable manner. The timeframe for the development of ISR is highly individual for each patient, and this can vary from weeks to months. Therefore, it is required that there are some key indicators to work from and use as a basis to help decipher when to initiate release for optimal efficacy.

### *5.3.1 Detecting onset of smooth muscle cell proliferation*

One of the most established and commonly used diagnostic tools for chronic inflammatory diseases is utilising MRI. With enhanced image quality, this gives informative assessments of the pathophysiology of the biological tissue and characterise inflammation within the vessel walls.

There have been advances in trying to improve the targeting of atherosclerosis using MRI markers. Some are aimed to target the cellular players within the vessel wall. At a molecular level, components that are identified as key biomarkers can target the main events of the atherosclerotic development; such as the inflammation and angiogenesis, oxidative stress, proliferation, and apoptosis (Letourneur, 2007). If specific MRI markers can indicate the onset of SMC proliferation at the early stages of ISR, this may provide the signal for initiating our drug release and this may be beneficial in investigating further.

Furthermore, since many of the cellular and molecular processes are mirrored in numerous other chronic disorders, any new diagnostic technology discovered for atherosclerosis will have a wider influence for the molecular imaging of many other chronic inflammatory diseases.

However, if we retrieve back to even earlier stages, and observe the blood-side events of atherosclerosis, there are some key markers circulating in the blood prior to the inflammation resulting in ISR. This includes; C-reactive protein, cell adhesion molecules, tumour necrosis factor-alpha, interleukins and soluble CD40 ligand (Letourneur, 2007). If introducing a new method that can enable detection of the

rising levels of these markers, such as through blood testing, it may be a feasible and simpler alternative to MRI imaging. To summarise, it is worthwhile to further investigate simpler and effective ways to detect the early stages of SMC proliferation.

### *5.3.2 Ultrasonic parameters influencing drug release*

One of the final aspects that require discussion is the ultrasonic conditions intended to be applied onto the device and to the patient. Primarily, these conditions must conform to the safety parameters of using ultrasound on individual patients, and to the safety threshold and restrictions within clinical settings.

There are also other influencing factors that need to be considered. The drug release profile can be heavily affected by the structure of the PE microcapsules themselves. As previously mentioned, the minimum number of PE layers required for stability is ten, with an optimum of fourteen to sixteen; any more layers render the microcapsules unstable. The number of layers is a determinant factor, with more layers constituting to an increased microcapsule thickness, and therefore requires more ultrasonic treatment to rupture the shells. Furthermore, the size of the initial core correlates to the amount of ultrasonic treatment required. Smaller cores have higher stability and are more resistant to the action of ultrasound (Kolesnikova *et al.,* 2008).

Finally, layers of metal inorganic nanoparticles significantly increase the sensitivity to ultrasound compared to solely PE microcapsules. When these entities are incorporated into the shell composition, layers become homogeneous. Combined with an increased total volume fraction, microcapsules have more elasticity, density, and therefore, mechanical strength (Kolesnikova *et al.,* 2008). A sharp increase in sensitivity occurs even when one layer is incorporated. Increasing this to two to five, the time required to completely rupture the microcapsules is between 2.5 to 4.5 minutes (Kolesnikova *et al.,* 2008). It should also be noted that it is not essential for the entire microcapsule to be destroyed to initiate leakage of the encapsulated material due to the exposed pores within the polymeric shells. Therefore, the effect

of high-frequency ultrasound is not only dependent on the total rupture, but on the perforation of the microcapsule wall (Pavlov *et al.*, 2011).

Particularly for cardiovascular applications, there have only been several publications to date regarding the use of ultrasonic release of substances from PE microcapsules and other nanocarriers. Studies revealed possible cardiac side effects provoked from using ultrasound treatment, such as induced bioeffects, premature contractions, and the potential to incite haemorrhages within the heart (Mayer and Bekeredjian, 2008). However, these *in vitro* studies utilised clinically irrelevant conditions which are unsuitable for *in vivo* applications. When comparable conditions were employed, the only side effect observed was an elevated level of Troponin T. Ultimately, this field still requires further research and development, utilising more clinically based parameters.

# 6 Conclusion

To collectively summarise, this thesis aimed to bring together an ideology to improve the current status of coronary DESs, and overcome the impeding disorders that followed after stent implantation. It was learnt within the literature review of the complexity the initial atherosclerotic formation presented, and of their therapeutic treatments. As these treatment modalities progressed from balloon angioplasty to BMSs to DESs, each has always presented a restricting limitation from fulfilling optimal patient outcomes; most predominantly, the pervasive ISR.

Drug-loaded PE microcapsules were suggested to encapsulate the drugs that coat stents, for the sole purpose of controlled drug release remotely. Although encountering difficulties in fabricating these microcapsules, with adequate improvements this project has the legitimacy to be taken forward and be developed into a medical device in its own right.

To conclude, it is important to revert back to the initial statistics. 17.3 million deaths and rising, are caused by CVDs every year with CAD responsible for over 40%. It is essential that the design and development of any new and improved cardiovascular device aim to reverse these statistics, and help influence an impact across the globe.

# 7 References


Acharya, G., & Park, K. (2006). Mechanisms of controlled drug release from drug-eluting stents. *Advanced drug delivery reviews*, *58*(3), 387–401.

Antipina, M. N., & Sukhorukov, G. B. (2011). Remote control over guidance and release properties of composite polyelectrolyte based capsules. *Advanced drug delivery reviews*, *63*(9), 716–29.

Anandhakumar, S., Debapriya, M., Nagaraja, V., & Raichur, A. M. (2011). Polyelectrolyte microcapsules for sustained delivery of water-soluble drugs. *Materials Science & Engineering C*, *31*(2), 342–349.

Bastus, N. G., Comenge, J., & Puntes, V. (2011). Kinetically Controlled Seeded Growth Synthesis of Citrate-Stabilized Gold Nanoparticles of up to 200 nm : Size Focusing versus Ostwald Ripening. *American chemical society*, 11098–11105.

Boudou, T., Kharkar, P., Jing, J., Guillot, R., Pignot-paintrand, I., Auzely-velty, R., & Picart, C. (2012). Polyelectrolyte multilayer nanoshells with hydrophobic nanodomains for delivery of Paclitaxel. *Journal of Controlled Release*, *159*(3), 403–412.

Chitkara, K., & Gershlick, A. (2010). Drug-eluting Stents Second- versus First-generation Drug-eluting Stents Drug-eluting Stents. *Interventional cardiology*, *5*(1), 23–26.

Dykman, L., & Khlebtsov, N. (2012). Gold nanoparticles in biomedical applications: recent advances and perspectives. *Chemical society review*, 2256–2282.

Farb, a., Heller, P. F., Shroff, S., Cheng, L., Kolodgie, F. D., Carter, a. J., Scott, D. S., et al. (2001). Pathological analysis of local delivery of paclitaxel via a polymer-coated stent. *Circulation*, *104*(4), 473–479.

Fessi, P., Alfort, M., Thies, C., & Louis, S. (1992). United States Patent Number 5118528.

Haude, M., Erbel, R., Issa, H., & Meyer, J. (1993). Quantitative analysis of elastic recoil after balloon angioplasty and after intracoronary implantation of balloon-expandable palmaz-schatz stents. *Journal of the American college of cardiology*, *21*(1), 26-34.

Huang, X., Jain, P. K., El-Sayed, I. H., & El-Sayed, M. a. (2007). Gold nanoparticles: interesting optical properties and recent applications in cancer diagnostics and therapy. *Nanomedicine (London, England)*, *2*(5), 681–93.

Kamath, K. R., Barry, J. J., & Miller, K. M. (2006). The Taxus drug-eluting stent: a new paradigm in controlled drug delivery. *Advanced drug delivery reviews*, *58*(3), 412–36.

Kolesnikova, T. A., Khlebtsov, B. N., Shchukin, D. G., & Gorin, D. A. (2008). Atomic Force Microscopy Characterization of Ultrasound-Sensitive Nanocomposite Microcapsules. *Nanotechnologies in Russia*, *3*(9-10), 560–569.

Lamalle-bernard, D., Munier, S., Compagnon, C., Charles, M., Kalyanaraman, V. S., Delair, T., Verrier, B., et al. (2006). Coadsorption of HIV-1 p24 and gp120 proteins to surfactant-free anionic PLA nanoparticles preserves antigenicity and immunogenicity. *Journal of controlled release*, *115*(1), 57–67.

Letourneur, D. (2007). Biomarkers of atherosclerosis and the potential of MRI for the diagnosis of vulnerable plaque. *Magnetic resonance materials in physics biology and medicine*, *3*(20).

Lévesque, J., Dubé, D., Fiset, M., & Mantovani, D. (2010). Materials and properties for coronary stents. *Advances materials & processes*, 45-48.

Lubell, D. L., Hospital, S., & To, I. (2002). Cardiology's 10 greatest discoveries. *Correspondence*, *29*(4), 342–344.

Mak, W. C., Cheung, K. Y., & Trau, D. (2008). Influence of different polyelectrolytes on layer-by-layer microcapsule properties : encapsulation efficiency and colloidal and temperature stability. *Chemical materials*, (8), 5475–5484.

Martin, D. M., & Boyle, F. J. (2011). Drug-eluting stents for coronary artery disease: a review. *Medical engineering & physics*, *33*(2), 148–63.

Mayer, C. R., & Bekeredjian, R. (2008). Ultrasonic gene and drug delivery to the cardiovascular system. *Advanced drug delivery reviews*, *60*, 1177–1192.

Mohan, D., & Dhall, A. (2010). A comparative study of restenosis rates in bare metal and drug-eluting stents. *International journal of angiology. 19*(2), 66-72.

Murakami, H., Kobayashi, M., Takeuchi, H., & Kawashima, Y. (1999). Preparation of poly(DL-lactide-co-glycolide) nanoparticles by modified spontaneous emulsification solvent diffusion method. *International journal of pharmaceutics*, *187*(2), 143–52.

Orozco, V. H., Kozlovskaya, V., Kharlampieva, E., López, B. L., & Tsukruk, V. V. (2010). Biodegradable self-reporting nanocomposite films of poly(lactic acid) nanoparticles engineered by layer-by-layer assembly. *Polymer*, *51*(18), 4127–4139.

Pavlov, A. M., Saez, V., Cobley, A., Graves, J., Sukhorukov, B., & Mason, T. J. (2011). Controlled protein release from microcapsules with composite shells using high frequency ultrasound — potential for in vivo medical use. *The royal society of chemistry, 7*(1), 4341–4347.

Rancan, F., Papakostas, D., Hadam, S., Hackbarth, S., Delair, T., Primard, C., Verrier, B., et al. (2009). Investigation of Polylactic Acid ( PLA ) Nanoparticles as Drug Delivery Systems for Local Dermatotherapy. *Pharmaceutical research, 26*(8), 2027-2036.

Ruggeri, G., Covolan, V. L., Bernabo, M., Li, L. M., Valadares, L. F., Leite, C. A. P., & Galembeck, F. (2013). Metal nanostructures with magnetic and biodegradable properties for medical applications. J*ournal of the Brazilian chemical society*, *24*(2), 191-200.

Schömig, A., Kastrati, A., & Wessely, R. (2005). Prevention of restenosis by systemic drug therapy: back to the future? *Circulation*, *112*(18), 2759–61.

Shi, W. T., Böhmer, M., Wamel, A. Van, Celebi, M., Emmer, M., Kooiman, K., Jong, N. De, et al. (2007). Ultrasound Therapy with Drug Loaded Microcapsules. *Ultrasonics symposium, IEEE*, 773–776.

Singh, M. T., Hemant, K. S., Ram, M., & Shivakumar, H. G. Microencapsulation: a promising technique for controlled drug delivery. *Research in pharmaceutical science, 5*(2), 65-77.

Skirtach, A. G., Geest, B. G. De, Mamedov, A., Antipov, A. A., Kotov, A., & Sukhorukov, G. B. (2007). Ultrasound stimulated release and catalysis using polyelectrolyte multilayer capsules. *Journal of materials chemistry*, *17*(1), 1050–1054.

Teirstein, P. S. (2010). Drug-eluting stent restenosis: an uncommon yet pervasive problem. *Circulation. 122*, 5–7.

Vergaro, V., Scarlino, F., Bellomo, C., Rinaldi, R., Vergara, D., Maffia, M., Baldassarre, F., et al. (2011). Drug-loaded polyelectrolyte microcapsules for sustained targeting of cancer cells. *Advanced drug delivery reviews*, *63*(9), 847–64.

**Websites**

[1] World Health Organisation statistics. Available at: http://www.who.int/topics/cardiovascular_diseases/en/

[2] Image of healthy and diseased coronary artery. Available at: http://www.northernsydneyvascular.com.au/PeripheralVascularDisease.html

[3] Medical treatments for coronary artery disease. Available at: http://www.nhlbi.nih.gov/health/health-topics/topics/cad/treatment.html

[4] Percutaneous coronary intervention and bare metal stent statistics. Available at: http://www.bcis.org.uk/pages/page_box_contents.asp?pageid=697&navcatid=11

[5] NHS coronary artery bypass graft statistics. Available at: http://www.nhs.uk/Conditions/Coronary-artery-bypass/Pages/Introduction.aspx

[6] Image of stent procedure within diseased coronary artery. Available at: http://www.britannica.com/EBchecked/topic/40908/atherosclerosis

[7] Image of drug-eluting stent drug release mechanism. Available at: http://www.medgadget.com/2009/08/zilver_ptx_drug_eluting_stent_for_peripheral_artery_disease_gets_european_approval.html

[8] Images of optical properties of gold nanoparticles (with permission). Available at: http://nanocomposix.com/kb/general/color-engineering

**Books**

Serruys, P. W., & Gershlick, A. H. (2005). Handbook of drug-eluting stents. ISBN 9781841841328